Title: A novel subset of follicular helper-like MAIT cells has capacity for B cell help and antibody production in the mucosa.

Author List: Owen Jensen[1,2], Shubhanshi Trivedi[1], Jeremy D. Meier[3,4], Keke Fairfax[2], J. Scott Hale[2], Daniel T. Leung[1,2*]

[1] Division of Infectious Diseases, Department of Internal Medicine, University of Utah School of Medicine, Salt Lake City, USA
[2] Division of Microbiology & Immunology, Department of Pathology, University of Utah School of Medicine, Salt Lake City, USA
[3] Division of Otolaryngology-Head and Neck Surgery, University of Utah School of Medicine, Salt Lake City, USA
[4] Primary Children's Hospital, Salt Lake City, USA

* Corresponding author: daniel.leung@utah.edu

One Sentence Summary: We identified and characterized a novel subset of T follicular helper-like MAIT (MAITfh) cells that has the capacity to provide B cell help, and show the sufficiency of MAIT cells to promote production of pathogen-specific IgA antibodies and B cell differentiation in mucosal challenge.

Abstract

Mucosal-associated invariant T (MAIT) cells are innate-like T lymphocytes that aid in protection against bacterial pathogens at mucosal surfaces via release of inflammatory cytokines and cytotoxic molecules. Recent evidence suggests MAITs are capable of providing B cell help. In this study, we describe a previously unreported population of $CXCR5^+$ T follicular helper (Tfh)-like MAIT cells, MAITfh, that have the capacity to provide B cell help within mucosal lymphoid organs. MAITfh cells are preferentially located near germinal centers in human tonsils and express the classical Tfh-associated transcription factor, B-cell lymphoma 6 (BCL-6), co-stimulatory markers, inducible T cell costimulatory (ICOS) and programmed death receptor 1 (PD-1), and cytokines, interleukin (IL)-21. Furthermore, we demonstrate the ability of MAITs to provide B cell help *in vivo* following mucosal challenge with *Vibrio cholerae*. Specifically, we show that adoptive transfer of MAITs into αβ T cell-deficient mice promoted B cell differentiation and increased serum *V. cholerae*-specific IgA and bactericidal responses. Our data demonstrate the capacity of MAITs to participate in adaptive immune responses, and suggest that MAITs may be potential targets for mucosal vaccines.

Introduction

Mucosal surfaces are in constant contact with both commensal and pathogenic microbes. One of the primary means of protection against invading pathogens is the production of secretory IgA and IgM by plasmablasts (PB) and plasma cells (PC) (*1*). In the lamina propria of the gut and lung, T independent low affinity IgA is produced against non-protein antigens by short-lived PBs. Conversely, T dependent high affinity antibodies against protein antigens are typically generated during germinal center reactions between T follicular helper (Tfh) and follicular B cells within local lymph nodes (LNs) or mucosal associated lymphoid tissues (MALT) (*2*). T follicular helper (Tfh) cells migrate to B cell follicles via upregulation of CXCR5 and downregulation of CCR7 (*3*). Within GCs, Tfh cells highly express the lineage-defining transcription factor, BCL6, and co-stimulatory molecules, PD1, ICOS, and CD40L (*4*). PD1 is important for Tfh GC positioning and function (*5*), while ICOS (*6*) and CD40L (*7*) engagement with B cells are essential for Tfh activation and GC formation (*4*). Tfh also produce cytokines, such as IL-21, that promote GC B cell responses (*8*).

Although Tfh cells are the primary drivers of T dependent GC responses, innate T cells, including invariant Natural Killer T (iNKT) cells and γδ T cells, also have Tfh like subsets capable of B cell help. In particular, iNKT cells have been well established in mice to provide both cognate and non-cognate help to B cells (*9–18*). Murine iNKTfh cells engage in cognate help leading to germinal center formation, and antibody class switching and production (*12*, *14*, *18*). iNKTfh cells have also been shown to promote non-cognate B cell help by licensing dendritic cells to recruit and activate Tfh cells (*10*, *11*). $CXCR5^+$ γδ T cells can promote antibody production *in vitro* (*19*, *20*), and promote Tfh differentiation *in vivo* (*21*). More recent evidence suggests that another type of innate-like lymphocyte, Mucosal-associated invariant T (MAIT) cells, are capable of B cell help (*22–26*).

MAIT cells are innate-like αβ T cells defined by the expression of an invariant α chain, generally Vα7.2 linked to Jα33, 12 or 20 in humans and Vα19 linked to Jα33 in mice, and a limited array of TCRβ chains (*27–29*). MAITs are highly enriched in human blood, liver and mucosa and are appreciated for their rapid ability to respond to microbial Vitamin B metabolites presented on the MHC class I related protein, MR1, or cytokine stimulation (*30–33*). Upon stimulation, MAITs produce pro-inflammatory cytokines including IFNγ, TNFα, and IL-17A and cytotoxic molecules including Granzyme B and Perforin (*34–36*). Furthermore, using MAIT deficient mice ($MR1^{-/-}$), several studies have exemplified the importance of MAITs in innate immunity against mucosal bacterial pathogens (*37–40*).

Recent evidence suggests MAITs play a role in adaptive immune responses through B cell help. Analysis of human peripheral blood MAITs and serum antibody responses following *Vibrio cholerae* infection (*22*) and *Shigella* vaccination (*35*), revealed strong associations between MAIT frequency and activation with polysaccharide-specific IgA and IgG responses, but not with protein antibody responses (*22*). We have recently shown that human blood MAITs have the capacity to induce antibody production and B cell differentiation *in vitro*, and can secrete the B cell help cytokines following stimulation (*23*). Analysis of pleural effusions from tuberculosis patients revealed a population of $PD1^{High}$ MAITs secreting key B cell help cytokines (*24*). Furthermore, two recent animal studies demonstrate the importance of MAITs in B cell help in murine autoimmunity (*25*) and mucosal vaccine immunity in non-human primates (*26*).

Our aims for this study were two-fold. We first wanted to determine whether a specific subset of MAIT cells are responsible for the B cell help phenotype. Our second aim was to determine *in vivo* if MAITs were sufficient to induce antibody production and humoral immune protection in the context of mucosal challenge. We found that like other innate-like T cells, MAITs have a Tfh like subset enriched within mucosal lymphoid organs. This MAITfh population expresses classical Tfh co-stimulatory markers, transcription factors, and cytokines, and is localized near B cell follicles. We further show, in a murine

model, that adoptively transferred MAITs are capable of generating protective antibody responses against mucosal bacterial pathogens in the absence of other αβ T cells. Additionally, we find that in the context of mucosal challenge, MAITs promote increased production of microbe-specific IgA antibodies and mucosal B cell differentiation. These results suggest that MAITs have the capacity to enhance mucosal antibody mediated immunity, and thus may be a prospective target in future mucosal vaccine development.

Results

CXCR5$^+$ MAITs are increased in tonsils and express higher levels of Tfh co-stimulatory markers compared to peripheral blood.

With recent evidence highlighting the ability of MAITs to provide B cell help, and studies showing a modest population of MAITs within human and mouse mucosal lymphoid tissues (*39*, *41*, *42*), we aimed to determine if MAITs had a Tfh-like subset capable of B cell help. To investigate this, we used flow cytometry to analyze MAIT expression of classical Tfh markers in human peripheral blood mononuclear cells (PBMCs) and tonsils. We obtained PBMC's from adult blood donors, and tonsils from children, ages 2-16, undergoing tonsillectomy for recurrent tonsillitis or tonsillar hyperplasia. MAITs were defined as CD3$^+$ Vα7.2$^+$ MR1-Tetramer$^+$ cells (Fig. 1A). Median MAIT frequency among total CD3$^+$ cells in tonsils was 0.23% (interquartile range (IQR) = 0.71%, 0.29%) compared to 1.03% (IQR = 0.62%, 1.35%) among PBMCs (Fig. 1B). We found that a higher percentage (Median=30%, IQR=10.36%, 42.5%) of tonsil MAITs were CXCR5$^+$ compared to PBMC MAITs (Median=1.74%, IQR=0.37%, 2.16%, $p<0.0001$), although there was significant variability among tonsil MAITs (Fig. 1C). We next wanted to determine if there were differences in Tfh co-stimulatory marker expression between CXCR5$^+$ and CXCR5$^-$ MAIT populations. CXCR5$^+$ MAITs in both tonsils and PMBC's had significantly higher ICOS (Fig. 1D) and PD1 (Fig. 1E) expression compared to CXCR5$^-$ MAITs of the same tissue. Additionally, CXCR5$^+$ MAITs in tonsils had significantly higher PD1 and ICOS expression compared to PBMC

CXCR5$^+$ MAITs. Notably, ICOS and PD1 frequency and fluorescence intensity among tonsil CXCR5$^+$ MAITs are similar to that seen in tonsil CD4$^+$ CXCR5$^+$ (Tfh) cells (data not shown). Taken together, a high proportion of MAIT cells in tonsils have a CXCR5$^+$ phenotype with Tfh-like co-stimulatory markers.

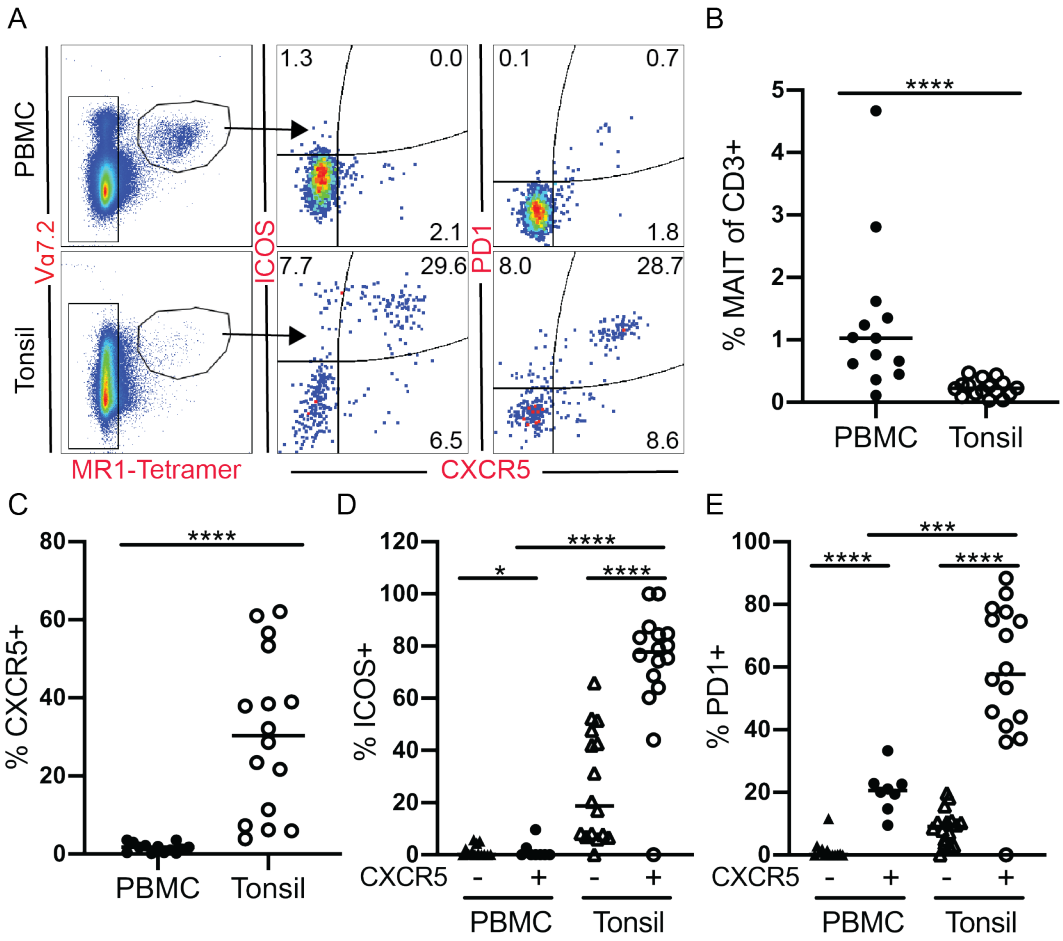

Fig. 1. Increased expression of Tfh co-stimulatory molecules in tonsil MAIT cells. (**A**) Representative FACS plots of unstimulated CD3$^+$ PBMC (top) and tonsil (bottom) cells with MAIT (gated in left panel) co-expression of CXCR5 with ICOS (middle) and PD1 (right). (**B**) Quantification of MAIT frequency as percentage of CD3$^+$. (**C**) Frequency of CXCR5$^+$ MAITs. Frequency of (**D**) ICOS$^+$ and (**E**) PD1$^+$ MAITs broken down by CXCR5 expression. Data are represented as median from 2 independent experiments. n ≥ 13. *$p < 0.05$, **$p<0.01$, ***$p<0.001$, ****$p<0.0001$ by two-tailed Mann-Whitney U test.

Transcriptional analyses of CXCR5$^+$ MAITs reveals expression of Tfh associated cytokines and transcription factors

We have previously demonstrated that peripheral blood MAITs can secrete B cell help cytokines IL-6, IL-10 and low levels of IL-21 *in vitro* (*23*). MAITs are also potent producers of IFNγ (*43*), which is known to have both inhibitory and activating roles in B cell development, proliferation, and antibody responses (*44*). In order to investigate the transcription factor and cytokine expression of CXCR5$^+$ and CXCR5$^-$ MAITs, we examined transcript levels of fluorescent associated cell sorted (FACS) MAIT and non-MAIT CD3$^+$ T cell populations from tonsil and blood. We refer to the sorted populations, as CD8$^+$ (CD8$^+$ CXCR5$^-$), Tfh (CD4$^+$ CXCR5$^+$), MAIT (MR1-Tet$^+$, Vα7.2$^+$, CXCR5$^-$), and MAITfh (MR1-Tet$^+$, Vα7.2$^+$, CXCR5$^+$) (fig. S1A). We first assayed for the Tfh lineage-defining transcription factor (TF), *BCL6*. The MAITfh population within PBMC and tonsils had higher *BCL6* expression compared to MAITs and Tfh cells. (Fig. 2A). In comparison, analysis of canonical T cell associated TFs *TBX21* (Th1) (p=0.03), and *RORC* (Th17) (p=0.03), revealed higher expression in tonsil MAITs over the tonsil MAITfh population (fig. S1B). Both MAIT and MAITfh groups had higher expression of *RORC* and *TBX21* compared to Tfh groups in PBMCs (MAIT:Tfh p=0.03, MAITfh:Tfh p=0.03) and tonsils (MAIT:Tfh p=0.03, MAITfh:Tfh p=0.03) (fig. S1B). Given that conventional Tfh cells are known to co-express TFs associated with other helper T cell subsets based on lineage and environment (*45–47*), our data suggest that co-expression of non-follicular helper-associated TFs in the MAITfh population may suggest potential for plasticity in phenotype or differentiation from a Th1, Th17 or CD8-like subset.

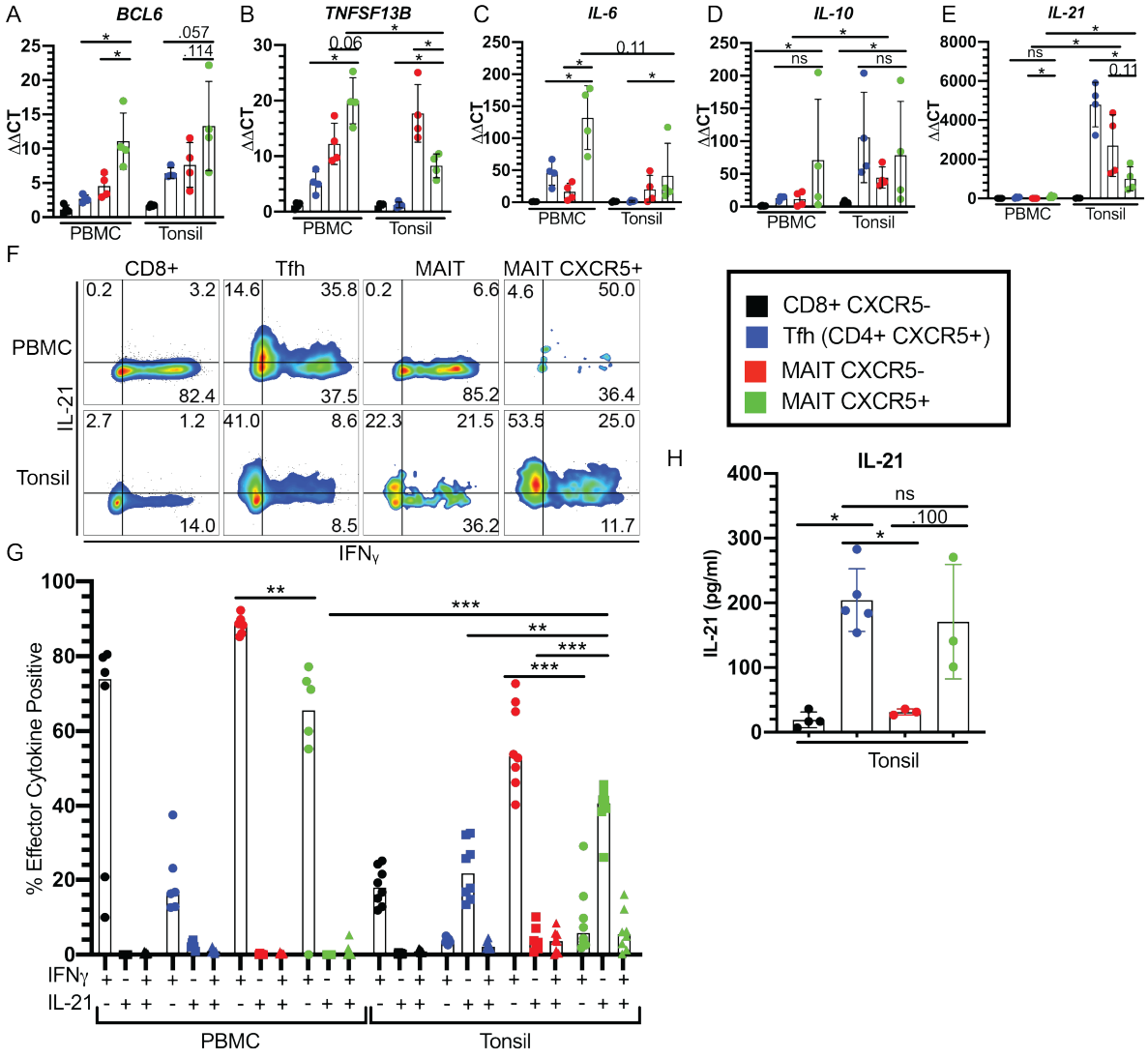

Fig. 2. CXCR5$^+$ MAITs highly express B cell help cytokine IL-21. (**A**) *Bcl6*, (**B**) *Tnfsf13b*, (**C**) *Il-6*, (**D**) *Il-10*, (**E**) *Il-21* qPCR data of unstimulated FAC sorted PBMC and tonsil T cell populations. Data are represented as ΔΔCt relative to an internal housekeeping gene, β-*Actin*, and the PBMC-CD8$^+$ CXCR5$^-$ population. (**F**) Representative flow cytometry from PBMC and tonsil T cell populations of IL-21 and IFNγ co-expression following 6 h stimulation with PMA/Ionomycin and Brefeldin A for final 4h. (**G**) Frequency of T cell populations expressing IL-21, IFNγ or both. Data are represented median from 2 independent experiments. n≥5. (**H**) IL-21 ELISA following 42 h PMA/Ionomycin stimulation of ≈40,000 FAC sorted mono-cultured T cell populations described below. Data are Mean with SD, n≥3. T cell populations described gated on live CD3$^+$ cells are as follows: Black =CD8$^+$ CXCR5$^-$, Blue = Tfh (CD4$^+$ CXCR5$^+$), Red= MAIT (MR1-Tetramer$^+$ Vα7.2$^+$) CXCR5$^-$, Green= MAIT CXCR5$^+$. Representative gating for populations found in Sup. Fig 1a. *$p < 0.05$, **$p<0.01$, ***$p<0.001$, ****$p<0.0001$ by two-tailed Mann-Whitney *U* test.

We next assayed for cytokines known to play a role in B cell differentiation or antibody production. *TNFSF13B (BAFF)* expression was significantly higher in both MAIT and MAITfh groups within tonsils and PBMCs compared to Tfh cells in their respective compartments (Fig. 2B). Similar results were seen in both *IL-10* (Fig. 2C) and *IL-6* (Fig. 2D) expression with trends of increased expression in MAITfh cells in PBMCs, though not in tonsils as there was significant variability between donors. Lastly, *IL-21* expression in tonsil MAITs and MAITfh, although 2-4 fold lower than tonsil Tfh cells, were highly elevated compared to corresponding populations in peripheral blood. Furthermore, the PBMC MAITfh population had a 46-fold and 2-fold enrichment in *IL-21* expression compared to the PBMC MAIT and Tfh populations, respectively (Fig. 2E). Taken together, CXCR5+ MAIT (MAITfh) cells express Tfh-associated cytokines and transcription factors at levels similar or higher than Tfh cells in their respective compartments

$CXCR5^+$ MAITs highly express IL-21 compared to $CXCR5^-$ MAITs

We next wanted to investigate the relationship between IL-21 and IFNγ expression among MAIT subsets as both cytokines are highly expressed and generally associated with a Tfh vs Th1 like phenotype. When we stimulated PBMCs with PMA/Ionomycin, we saw a clear dichotomy between IFNγ and IL-21 positive cells in all populations with very low frequency of double positive cells, and the vast majority being $IFN\gamma^+$ (Fig. 2 F and G). MAITfh had a significantly lower frequency of $IFN\gamma^+$ cells compared to conventional MAITs ($p<0.01$). This effect was even more notable in tonsils ($p<0.001$), where IFNγ production was significantly reduced compared to that of PBMCs ($p<0.001$), with a similar dichotomy between IFNγ-expressing MAITs and IL-21-expressing MAITfh. Furthermore, the tonsil MAITfh population had a significantly ($p<0.01$) higher frequency of $IL\text{-}21^+$ cells compared to conventional Tfh cells following stimulation (Fig. 2F and G). Conversely, $IFN\gamma^+$ frequency is low in all unstimulated populations but increases drastically in the tonsil MAIT population from >1% to approximately 88% following stimulation (fig. S2 A and B). To confirm the IL-21 production capacity of MAITs and

MAITfh cells within tonsils, we sorted MAITs ($CD3^+$ $V\alpha7.2^+$ MR1-Tetramer$^+$ $CXCR5^-$), MAITfh ($CD3^+$ $V\alpha7.2^+$ MR1-Tetramer$^+$ $CXCR5^+$), $CD8^+$ $CXCR5^-$ and GC Tfh ($CD4^+$ $CXCR5^+$ $PD1^{high}$) populations, and stimulated mono-cultures of these cells with PMA/Ionomycin (*48*). We found higher IL-21 production in the MAITfh over MAIT groups and no statistical difference in IL-21 production between MAITfh and GC Tfh populations (Fig. 2H). In addition, we found an increase in frequency of IL-6 and IL-10 positive cells following stimulation (fig. S2 C and D), concordant with what was found with qPCR analysis above. Taken together, these data demonstrate the potent ability of the tonsil MAITfh population to produce B-cell help cytokines and the clear dichotomy in phenotype between classical MAITs and MAITfh cells in both peripheral blood and tonsil tissue.

$PD1^+$ MAITs localize near germinal centers within tonsils

Having established that $CXCR5^+$ MAITs exhibit a Tfh-like phenotype *in vitro*, we next sought to determine the *in vivo* spatial differences between CXCR5- and CXCR5+ MAITs in relation to germinal centers (GCs) in tonsil cryosections. MAITs were defined by co-staining of TRAV1-2 and CD161 as described in Leng et al. 2019 (*49*). IgD was used to stain naïve B cells making up the follicular mantle, and potential IgD+ memory B cells in the marginal or superficial zone (*50*). Due to difficulties with co-staining MAITs and CXCR5, we used PD1 to mark MAITfh and non-MAIT GC Tfh cells. PD1 has been used to mark GC light zone Tfh cells in non-human primates (*51*), and further analyses of flow cytometry data (Fig. 1) verify a strong correlation ($r=0.9373$, $p<0.001$) between $PD1^+$ and $CXCR5^+$ percent frequencies in tonsil MAITs (Fig. 3A). Additional analyses confirm that a median of 92% (IQR=78.03%, 92.18%) of $PD1^+$ MAITs are $CXCR5^+$, compared to a median of 15% (IQR=13.18%, 23.1%) for $PD1^-$ tonsil MAITs (Fig. 3B). ImageJ was used to quantify and measure $PD1^{+/-}$ MAIT distance to the edge of the nearest GC, outlined in Fig. 3C (dashed white line). A total of 349 MAITs from n=5 tonsils were analyzed with 32% ± 15.9 being $PD1^+$. In comparison, flow results of unstimulated tonsil cells showed 38% ± 14.9 of MAITs to be $PD1^+$, thus confirming the ability of the immunohistochemistry imaging and

quantification to assess this cell population. $PD1^{+}$ MAITs were generally located within or closely surrounding GC's with a median distance of 66.8 μm from a GC edge compared to $PD1^{-}$ MAITs with a median distance of 220.2 μm (Fig. 3D). 28.4% of $PD1^{+}$ MAITs were located within GC's and thus were recorded as 0 μm. $PD1^{High}$ expressing MAITs tended to localize with other $PD1^{High}$ cells within GC light zones. In contrast, $PD1^{low}$ or $PD1^{-}$ MAITs were often found outside of the IgD^{high} follicular mantle zone (Fig 3C-yellow dashed line) and frequently in contact with IgD^{low} cells. Overall, combined with phenotypic analysis above, these data reveal $PD1^{+}$ (and likely $CXCR5^{+}$) MAIT cells to be Tfh-like in their proximity to germinal centers.

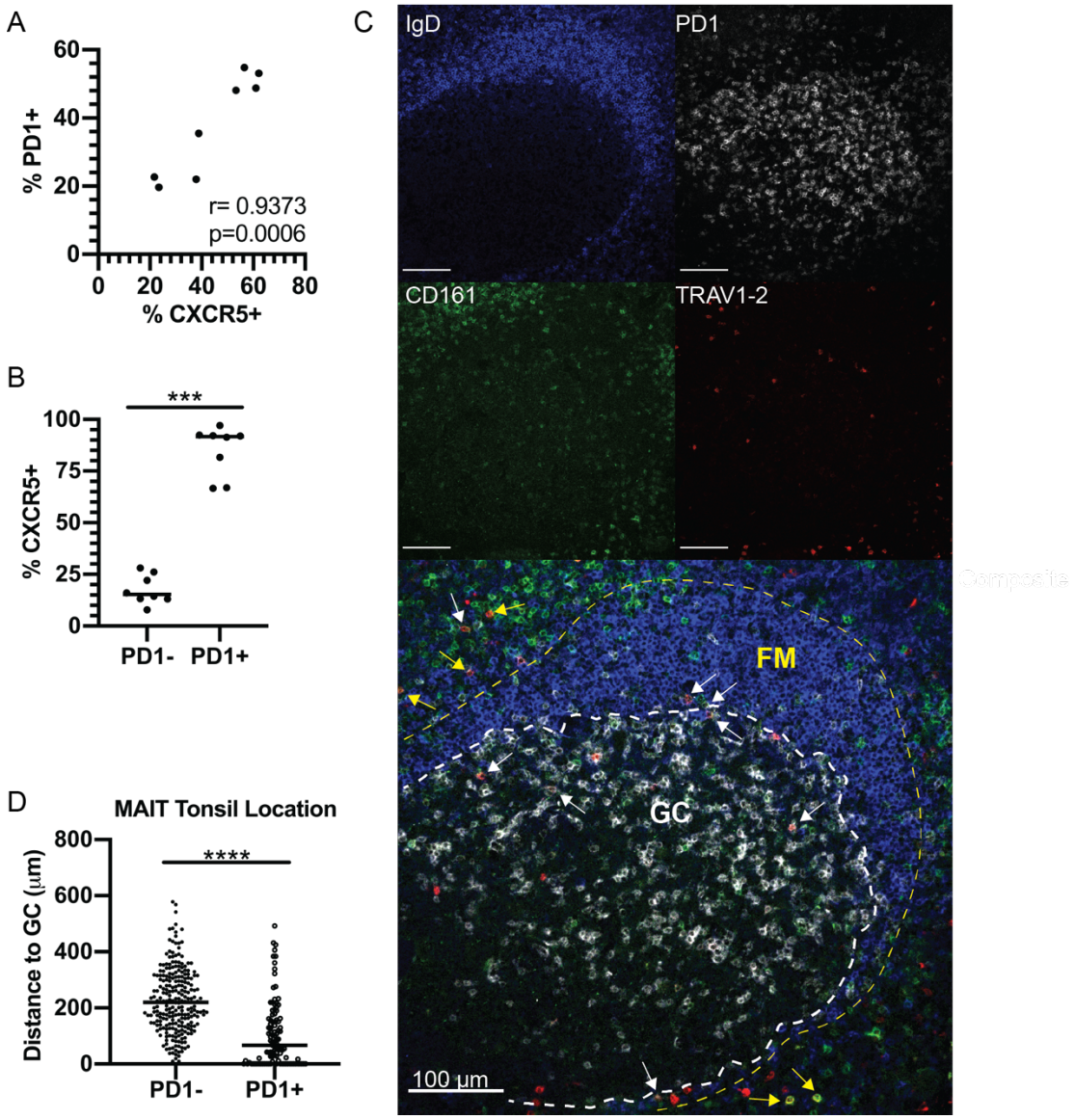

Fig. 3. PD1^{high} MAITs preferentially locate near B cell follicles. (**A-B**) Association between PD1 and CXCR5 expression among tonsil MAITs by flow cytometry. Data were analyzed by Spearman correlation test (**A**), and two-tailed Mann-Whitney *U* test (**B**). *$p < 0.05$, **$p<0.01$, ***$p<0.001$, ****$p<0.0001$. (C) Location of MAIT cells within tonsils. Representative immunofluorescence images from tonsil cryosections stained with IgD (blue), PD1 (white), CD161 (green), and TRAV1-2 (red) and imaged on a Leica SP8 confocal microscope with 20X objective. Enlarged composite image on right with MAIT cells (TRAV1-2$^+$ CD161$^+$) denoted with arrows. White arrows indicate PD1$^+$ MAITs. Yellow arrows indicate PD1$^-$ MAITs. White dashed line outlines germinal center (GC) highlighted by PD1^{high} cells. Yellow dashed line outlines follicular mantle (FM) highlighted by IgD$^+$ naïve B cells. All scale bars represent 100 µm. (**D**) Quantification of MAIT distance to edge of nearest GC. Tiled images from tonsil donors were visually assessed for co-staining of CD161, TRAV1-2 and then PD1. Distance to nearest GC was then measured using ImageJ. n=359 MAITs were quantified (PD1$^+$ = 103; PD1$^-$ = 246) from n=5 tonsil donors. Data are represented as medians with dots representing single MAIT cells. *$p < 0.05$, **$p<0.01$, ***$p<0.001$, ****$p<0.0001$ by two-tailed Mann-Whitney *U* test.

Varied transcription factor profile despite similar TCR sequence variability in tonsil and PBMC MAITs

Human MAITs are defined by their invariant TCR-Vα chain, with the vast majority (>99%) being Vα7.2 or TRAV1-2, though recent studies suggest variability in TRAJ sequence and TRBV usage affects microbial ligand discrimination, activation, and phenotype (*36*, *52*, *53*). Despite this, few studies have analyzed MAIT TCR sequences from tissue (*54–56*), with limited sequence analysis in lymphoid organs (*29*, *56*). Therefore, to determine whether differences in TCR sequence between peripheral and lymphoid associated MAITs may direct phenotype, we utilized paired TCR-phenotype single-cell Illumina sequencing as previously described (*57*). We sorted and single-cell sequenced MAIT cells (identified as live $CD3^+$ $V\alpha7.2^+$ MR1-$Tetramer^+$ cells) from tonsil samples and PBMCs. We first analyzed *TRAJ* and *TRBV* usage frequency by donor, finding similar inter-donor profiles among tonsil and PBMC MAITs (Fig. 4A and fig. S3A). In concurrence with previous studies (*29*, *54*, *56*, *58*), the majority of PBMC and tonsil MAITs express *TRAJ-33* along with *TRBV 20-1*, *6-1*, or *6-4*. Although not statistically significant (when correcting for multiple comparisons), we found an increase in *TRAJ 12* and *34* frequency (fig. S3A), a decrease in *TRBV 20-1*, and an increase *TRBV 7-2* in tonsil versus PBMC MAITs (Fig. 4A). Furthermore, consensus TRA and TRB sequences, represented using Seq2logo, show little variation between tonsil and PBMC MAIT CDR3 sequences (fig. S3B). Thus, despite differences in age and anatomical location, blood and tonsil MAITs share similar TCR usage. Despite significant overlap in *TRAJ* and *TRBV* usage between blood and tonsil MAITs, analysis of TCR sequences suggested higher number of unique MAIT clones within the tonsil samples compared to PBMCs (Fig. 4B), though this difference could potentially be attributed to age difference in donors, as older adults tend to have more clonally expanded MAIT populations (*56*). In addition to TCR sequence analysis, we further measured, at the single-cell level, expression of key transcription factors associated with T helper subsets and CD8 T cells, *RORC, TBX21, BCL6, GATA3* and *RUNX3*, using targeted primers (Fig. 4C). While we found no difference in the frequency of expression of the Th17 and Th1-associated transcription factors, *RORC* and

TBX21, we found an increase in the Tfh lineage defining transcription factor, *BCL6*, in tonsil relative to PBMC MAITs. Interestingly, substantial increases in the Th2-assoicated transcription factor, *GATA3,* and resident CD8 T cell associated transcription factor, *RUNX3* were also observed. These data corroborate RT-qPCR data showing higher *BCL6* and *RUNX3* expression in tonsil compared to PBMC MAITs and MAITfh cells, and similar *RORC* and *TBX21* expression (Fig. 2a, and fig. S1B). No associations were observed between *TRBV* usage and transcription factor expression and phenotype (data not shown). These data suggest that TCR variability is not directly related to MAIT phenotype.

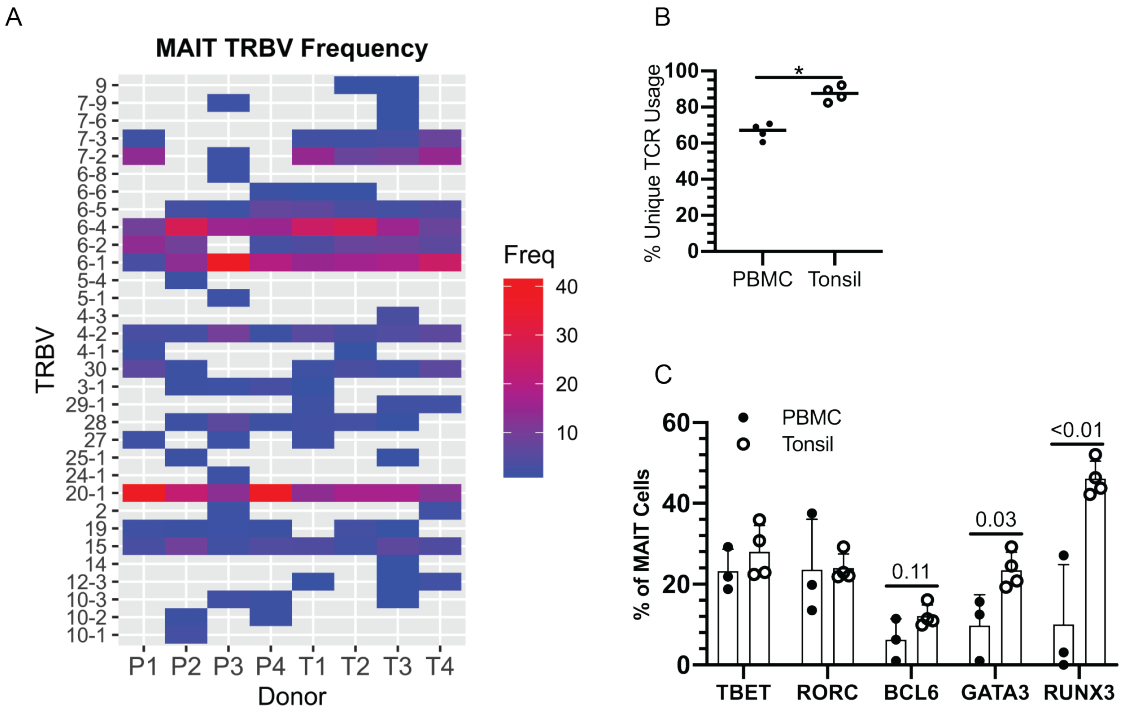

Fig. 4. Overlapping TRBV usage between blood and tonsil MAITs despite transcription factor variance. (**A**) Heat map of TRBV usage percent frequencies based on Illumina single cell TCR-Phenotype sequencing in tonsil and PBMC MAITs. Each column represents an individual donor (n=4). No statistical significance was found between tonsil and PBMC groups using Multiple t tests comparison accounting for False Discoveries using the Benjamini, Krieger and Yekutieli method. (**B**) Frequency of unique TCR usage (non-clonally expanded) within PBMC and tonsil MAITs. The frequencies of non-repeating TCR usage based on TRA and TRB sequence per donor were calculated using R. Data are medians. n=4. (**C**) Targeted single-cell transcription factor expression sequencing in PBMC and tonsil MAITs. Data are represented as frequency of MAIT cells expressing each gene per donor. Data are mean with SD. n≥3. *$p < 0.033$, *$p < 0.05$, **$p<0.01$, ***$p<0.001$, ****$p<0.0001$ by two-tailed Mann-Whitney *U* test (B) or Multiple students t-tests (C).

MAITs repopulate mucosal and lymphoid organs following adoptive transfer in TCRα$^{-/-}$ mice

To study the sufficiency of MAITs to provide B cell help in the context of mucosal immune responses *in vivo*, we utilized an adoptive MAIT transfer model into T*cra*^{tm1Mom}/J (TCRα$^{-/-}$) mice followed by a prime-boost model of mucosal bacterial infection. Expansion of lung MAITs from WT C57Bl/6 (B6) mice using an intranasal *Salmonella* Typhimurium challenge have shown to result in MAIT cells that retain function even after adoptive transfer (*40*). TCRα$^{-/-}$ mice have been successfully used in T cell transfer experiments to study the B cell help potential of non-Tfh CD4 T cells without the potential masking effects of classic Tfh cells (*59*). We thus adoptively transferred expanded lung MAITs from B6 into TCRα$^{-/-}$ mice and then utilized an intranasal prime-boost challenge model with live *Vibrio cholerae* O1 Inaba (*V.c*) that induces systemic and mucosal LPS IgA and IgG responses (*60*) (Fig. 5A). To confirm MAITs were successfully transferred into recipient mice, we measured MAIT frequencies and total cell numbers by flow cytometry of digested lung tissue and spleen (Fig. 5B and fig. S4A-C). The frequency and total cell count of lung MAITs at Day 42 in MAIT-*V.c* and MAIT-PBS groups were statistically similar to the WT- *V.c* group (Fig 5C and fig. S4B). Importantly, no MAITs were recorded in either Sham-*V.c* or Sham-PBS group. Similar MAIT cell counts were also observed in the spleen (fig. S4C), thus demonstrating WT physiologic MAIT frequencies and repopulation of various organs following adoptive transfer of lung MAITs. Furthermore, we found no differences between all TCRα$^{-/-}$ groups in total non-MAIT TCRβ+ T cells, thus confirming no significant expansion of contaminating non-MAIT T cells following adoptive transfer (fig. S4D). We next analyzed the expression of CXCR5 in CD8 T cells, CD4 T cells and MAIT cells in the WT-*V.c* and MAIT-*V.c* groups (Fig. 5D and E). MAITs from both WT-*V.c* and MAIT-*V.c* mice showed no statistical difference in CXCR5 expression when compared to CD4 T cell populations in lungs suggesting a potential mouse MAITfh population (Fig. 5D and E). Taken together, we found that adoptive transfer of expanded MAIT cells into TCRα$^{-/-}$ mice repopulates MAIT cells, including CXCR5+ MAITs, in lymphoid and mucosal organs, to levels similar to that of WT mice.

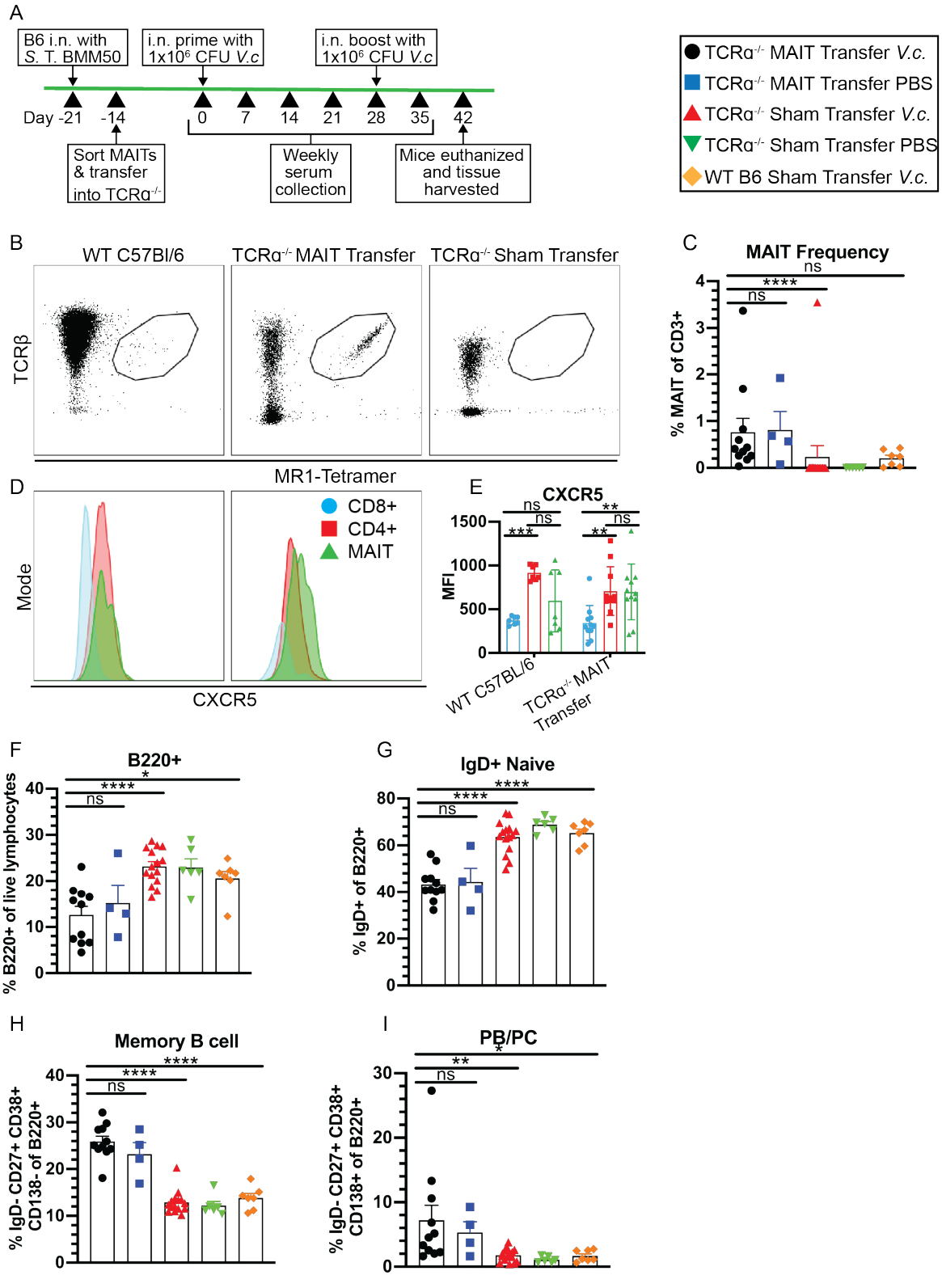

Fig. 5. Adoptively transferred MAITs expand in lungs of TCRα$^{-/-}$ mice driving B cell differentiation. (**A**) MAIT adoptive transfer and *V.c* intranasal challenge time-line. (**B**) Representative FACS plots of MAITs (TCRβ^{+} MR1-Tetramer^{+}) from lung tissue of WT-*V.c* (left), MAIT-*V.c* (middle), and Sham-*V.c* (right) mice at Day 42 post initial *V. cholerae* challenge. (**C**) MAIT frequency as percentage of CD3^{+}. Representative flow cytometry histograms (**D**) and Mean fluorescence intensity quantification (**E**) of CXCR5 in non-MAIT CD8 T cells (blue), non-MAIT CD4 T cells (red) and MAIT cells (green) of WT-*V.c* (left) and MAIT-*V.c* (right) groups. (**F**) Frequency of B220^{+} B cells among live lymphocytes. Frequency of IgD^{+} naïve B cells (**G**), IgD^{-} CD27^{+} CD38^{+} CD138^{-} Memory B cells (**H**) and IgD^{-} CD27^{+} CD38^{+} CD138^{++} PB/PCs (**I**) as percent of B220$^{low\text{-}high}$ lymphocytes. Data are represented as Mean with SEM from 4 independent experiments. n= 4-15 mice per group. *$p < 0.05$, **$p<0.01$, ***$p<0.001$, ****$p<0.0001$ by two-tailed Mann-Whitney *U* test. Legend in black box denotes experimental groups: MAIT-*V.c* = TCRα$^{-/-}$ plus MAIT Transfer-*V.c* challenge, MAIT-PBS = TCRα$^{-/-}$ plus MAIT Transfer-PBS challenge, Sham-*V.c* = TCRα$^{-/-}$ plus Sham Transfer-*V.c* challenge, Sham-PBS = TCRα$^{-/-}$ plus Sham Transfer-PBS challenge, WT-*V.c* = WT C57Bl/6J plus Sham Transfer-*V.c* challenge.

MAIT transfer drives increase in plasmablast differentiation and memory B cell development

We next sought to determine the impact of MAIT adoptive transfer on mucosal B cell differentiation. Day 42 digested lung suspensions were analyzed by flow cytometry with B cells being defined as B220+ lymphocytes. Interestingly, total B220+ cell frequency (Fig. 5F) and total B cell count per lung (fig. S4E) were decreased in both the MAIT-*V.c* and MAIT-PBS groups compared to Sham-*V.c*, Sham-PBS and WT-*V.c* groups. Similar decreases in IgD^{+} naïve B cell frequency were observed in MAIT transfer groups (Fig. 5G), although no statistical differences were observed in total naïve B cells (fig. S4F). In contrast, we found that both MAIT-*V.c* and MAIT-PBS groups had higher Memory B cell (B220+ IgD- CD27mid CD38+ CD138-) and Plasmablast(PB)/Plasma cell (PC) (B220low IgD- CD27+ CD38+ CD138++) frequency as a percentage of total B cells compared to Sham-*V.c,* Sham-PBS and WT-*V.c* groups (Fig. 5H and I). Total Memory B cell count per lung was not statistically different between groups with significant variability observed in the MAIT-*V.c* group (fig. S4G), though we saw a non-statistically significant higher total PB/PC cell count per lung in MAIT-*V.c* compared to Sham-*V.c* (p=0.097) and WT-*V.c* (p=0.179) groups (fig. S4H). Overall, these data suggest that in the absence of αβ T cells, transfer of activated MAITs help induce B cell differentiation from naïve B cells to PB/PCs or memory B cells.

Increase in V. cholerae specific IgA responses and vibriocidal titer following MAIT transfer

V.c-specific antibodies in blood is a surrogate for protection against cholera (*61*, *62*). Specifically, the vibriocidal assay, a measurement of complement-fixing bactericidal antibody activity, has been in use since the mid twentieth century (*63*) and shown to be the best marker of protection (*64*, *65*). In addition to the vibriocidal titer, cholera toxin (CT) and lipopolysaccharide (LPS) serum ELISAs have been widely used to estimate cholera incidence (*65–68*). The O-specific polysaccharide (OSP) component of LPS and CT are the immunodominant antigens following cholera infection (*69*). Therefore, in order to measure the impact of MAIT transfer on pathogen-specific antibody kinetics we measured serum IgG, IgA, and IgM antibody responses against whole *V.c*-lysate, OSP, and CT. We found comparable *V.c*-lysate IgA responses in the MAIT-*V.c* and WT-*V.c* groups particularly following *V.c* re-challenge (D28), suggesting development of a memory response (Fig. 6A). Day 42 endpoint ELISAs reveal a substantial increase in *V.c*-lysate IgA responses in the MAIT-*V.c* group compared to Sham-*V.c* ($p<.0001$), and a non-statistically significant increase ($p = 0.58$) compared to the WT-*V.c* group (Fig. 6C). Importantly, minimal *V.c*-lysate IgA responses were observed in the Sham-PBS group. MAIT-*V.c* and MAIT-PBS groups had no differences in *V.c*-lysate IgG (Fig. 6B and D) and IgM (fig. S5A and B) responses, despite an increase compared to Sham transfer groups, thus indicating a non-specific response induced by MAIT transfer. We saw a non-significant ($p=0.054$) increase in OSP IgA responses in the MAIT-*V.c.* group compared to the Sham-*V.c* group (Fig. 6E and G), but no differences on OSP-IgG responses (Fig. 6F and H). Notably, even Sham-infected TCRα-/- mice were able to mount (albeit lower than WT) OSP IgG responses, indicating that a lack of T cells blunted, but did not eliminate, the ability to mount an IgG response to a polysaccharide antigen, which is classically T-independent. In contrast, OSP-IgM levels were similar between the MAIT-*V.c*, Sham-*V.c*, and WT-*V.c* groups, and all were increased compared to MAIT-PBS and Sham-PBS groups indicating a specific but truly T-independent response (fig. S5E and F). Overall, very low levels of CT IgA and IgG were observed in all TCR$\alpha^{-/-}$ groups (Fig. 6I-L) compared to the WT-

V.c group, supporting the role of classical helper T cells in protein antigen B cell help, a response that adoptive transfer of MAIT cells did not rescue. Analysis of total serum IgA revealed a highly variable but substantial increase in both MAIT transfer groups over both Sham transfer and WT-*V.c* groups (fig. S5H). No statistically significant changes were observed in total IgM and IgG between MAIT-*V.c* and Sham-*V.c* groups (fig. S5G and I).

We further utilized the vibriocidal assay to measure complement-mediated bactericidal activity, the best studied and most commonly used correlate of protection from cholera in humans (*64*, *65*). We found an increase in vibriocidal titer in the MAIT-*V.c* group compared to the Sham-*V.c* group ($p=0.069$), and no difference when compared to the WT-*V.c* group, suggesting MAIT transfer is sufficient to rescue vibriocidal responses (Fig. 6M). Unlike the ELISAs, no background vibriocidal responses were observed in the MAIT-PBS group demonstrating the specificity of this assay. Taken together, adoptive transfer of MAIT cells into T-cell deficient mice rescued deficiencies in *V. cholerae*-specific IgA and vibriocidal antibody responses.

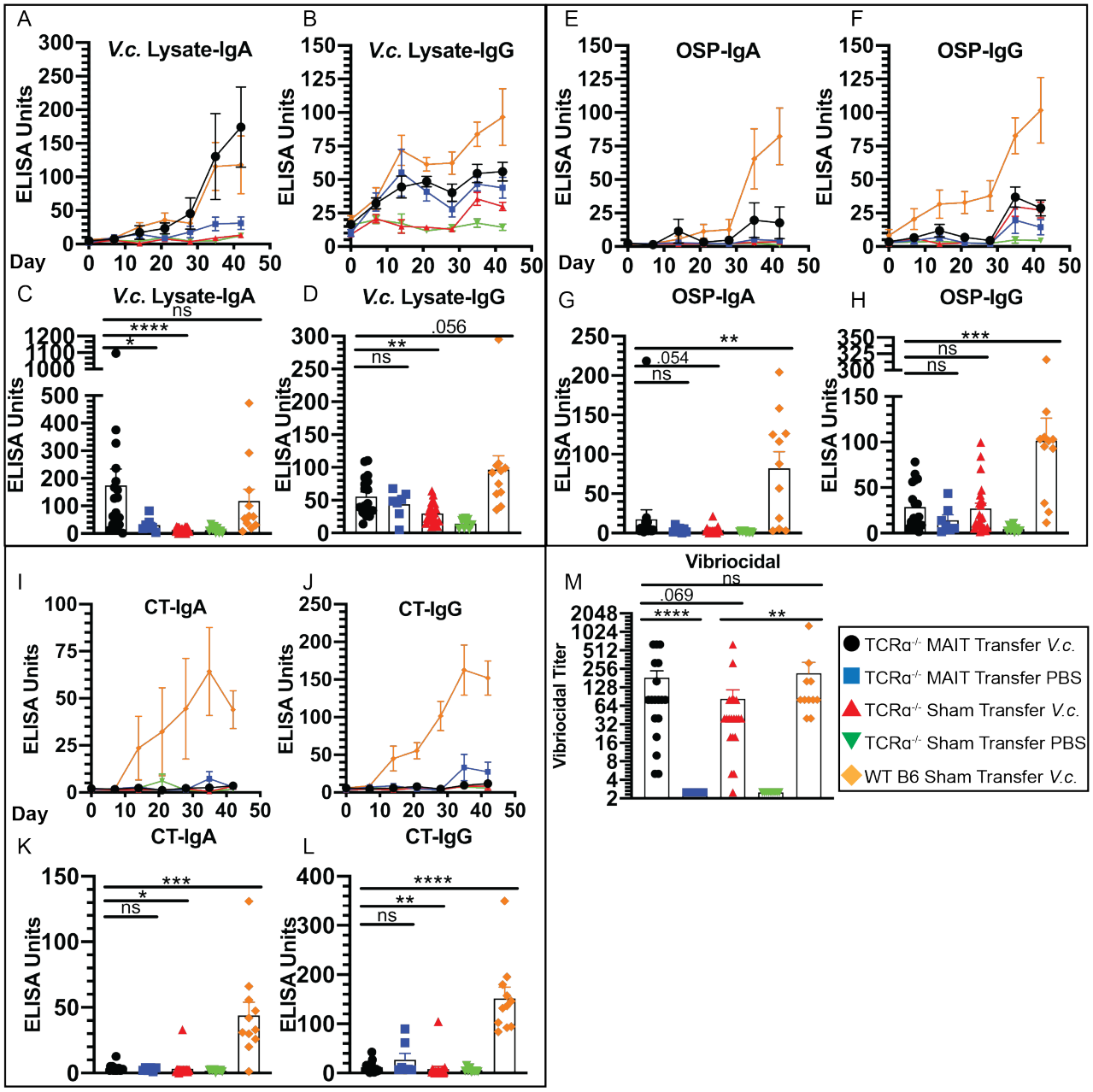

Fig. 6. MAITs promote *V. cholerae*-specific IgA and protective vibriocidal antibody responses in TCRα$^{-/-}$ mice. Serum ELISAs against *V. cholerae* whole lysate, OSP and CT. (**A-D**) IgA and IgG *V. cholerae* lysate ELISAs from weekly cheek bleed (A & B) and Day 42 endpoint serum (C & D). (**E-H**) IgA and IgG OSP ELISAs from weekly cheek bleed (E & G) and Day 42 endpoint serum (F & H). (**I-L**) IgA and IgG CT ELISAs from weekly cheek bleed (I & J) and Day 42 endpoint serum (K & L). Data are represented as ELISA units normalized to a pooled serum positive control from WT B6 mice challenged with *V. cholerae*. (**M**) Vibriocidal titer of Day 42 endpoint serum. Data are represented as Mean with SEM from 5 independent experiments. n= 6-22 mice per group. *$p < 0.05$, **$p<0.01$, ***$p<0.001$, ****$p<0.0001$ by two-tailed Mann-Whitney *U* test. Legend in black box denotes experimental groups.

Discussion

MAIT cells are widely appreciated for their ability to respond rapidly to microbial antigens and cytokines through potent production of Th1 and Th17-associated inflammatory cytokines and cytotoxic molecules. Recent studies have highlighted the capacity of human MAITs to provide B cell help *in vitro*, and promote B cell differentiation and antibody production in animal models (*23*, *25*, *26*). Despite these findings, whether there remains a pre-defined MAIT subset capable of B cell help remains uncertain. Additionally, many studies have detected MAITs within mucosal lymphoid tissues but have yet to understand their role in these environments (*33*, *41*, *70*). In this study we begin to define the role of MAITs in human mucosal lymphoid organs and uncover a novel T follicular helper-like MAIT population defined by CXCR5. This MAITfh subset highly expresses PD1, ICOS, *BCL6*, and IL-21, and preferentially locates near germinal centers. We further add to the body of literature proving the ability of MAITs to provide B cell help *in vivo* through sufficiency experiments following mucosal challenge. Here we show that adoptively transferred MAITs can rescue protective microbe specific responses, and promote B cell differentiation in the absence of other αβ T lymphocytes.

We report a subset of $CXCR5^+$ MAIT (MAITfh) cells that are enriched in mucosal lymphoid organs and represent a small percentage of peripheral blood MAITs (Fig. 1C). We further report that MAITfh cells highly express the B cell help co-stimulatory molecules, PD1 and ICOS, compared to $CXCR5^-$ MAIT cells (Fig 1D and E). In addition, we show high relative expression (≈20-70 fold) of *CD40L* in both MAITs and MAITfh groups compared to the control CD8+ population (fig. S1B). PD1, ICOS and CD40L expression are a hallmark of GC Tfh cells (*71*). PD1, although long considered a marker of T cell exhaustion, has an important role in Tfh GC positioning and function (*5*). ICOS and CD40L engagement with ICOS Ligand and CD40 expressed on B cells is essential for GC formation and Tfh activation (*6*, *7*). CD40L is also implicated in MAIT induced maturation of dendritic cells (*72*). Based on the Tfh costimulatory molecule profile, we hypothesized that MAITfh cells may share further transcriptional

similarities with Tfh cells. In support, we found that MAITfh cells in tonsils and PBMCs have higher *BCL6* expression than MAITs and Tfh cells in both PBMCs and tonsils (Fig. 2A). Additionally, we reported more *BCL6*$^{+}$ MAITs in tonsils relative to PBMC MAITs (Fig. 4C). BCL6 is considered the master regulator of the Tfh lineage (*73*) and is similarly required for iNKTfh B cell help responses (*18*). Furthermore, expression of *BLIMP1*, which is a negative regulator of Tfh differentiation (*73*) was lower in the tonsil MAITfh vs MAIT groups. Although further research into the transcriptional regulation of MAITfh cells is necessary to understand the requirements for differentiation, plasticity and function, these data support a B cell help transcriptional phenotype among the MAITfh subset.

We report MAITfh expression of the B cell help cytokines IL-21, IL-10, IL-6 and *BAFF* (Fig. 2 and fig. S2). IL-21 and IL-10 were specifically upregulated in MAITfh cells, while *BAFF* and IL-6 were also highly expressed in both PBMC and tonsil MAIT cells compared to CD8 controls. IL-21 plays an important role in T dependent B cell differentiation, class switching and antibody production (*74*) and together with IL-6 promotes Tfh differentiation (*75*). IL-10 promotes antibody production and class switching (*76*). IL-21 expression in MAITs has been demonstrated in low concentrations in PBMC MAITs (*23*), and in a subset of PD1^{High} CXCR5- MAITs in pleural effusions from Tuberculosis patients (*24*). This study also presents a small subset of CXCR5^{+} PD1^{high} MAITs, though they do not investigate whether this population expressed IL-21 as well (*24*). In contrast, we show that tonsil CXCR5^{+} MAITs are largely IL-21^{+} IFNγ^{-} (Fig. 2G) and produce significantly more IL-21 than CXCR5^{-} MAITs (Fig. 2H). It is unclear whether PD1^{High} CXCR5^{-} MAITs in pleural effusions are transcriptionally or developmentally related as potential precursors to CXCR5^{+} MAITs found in lymphoid tissues. Furthermore, the B cell survival cytokine, BAFF, is integral in T independent class switching and differentiation (*77*), and is similarly produced by iNKTfh cells to promote B cell responses (*18*). Thus, it is possible MAITfh cells can aid in B cell help through cognate interactions via direct MR1-TCR, co-stimulatory molecule engagement and cytokine expression, or through non-cognate interactions such as promoting Tfh differentiation or licensing of dendritic cells.

We have observed that PD1^{high} MAITs preferentially locate within or around GCs in human tonsils (Fig. 3C and D). We further prove these cells are likely CXCR5^{+} based on high co-expression with PD1 (Fig. 3A and B). This is noteworthy since spatial positioning of T and B cells within lymphoid tissues is critical in understanding their phenotype. For instance, CXCR5^{+} PD1^{High} GC Tfh cells reside primarily in the light zone of GCs where they promote affinity maturation and differentiation of GC B cells leading to high affinity antibody responses (*71*). Thus, by combining imaging results with *in vitro* MAITfh expression of B cell help co-stimulatory markers and cytokines (Fig. 1 and 2), we can conclude that MAITfh cells share both phenotype and positioning with traditional GC Tfh cells. Thus we hypothesize that this population may be involved in cognate or contact-dependent B cell help as is seen in other innate Tfh subsets, such as iNKTfh (*12*). Though as this population is relatively small in tonsils, further research will need to address the *in vivo* relevance to overall mucosal antibody production, the role of MAITfh-B cell interactions in affinity maturation, and development of B cell memory.

We report that adoptive transfer of murine MAITs boosts pathogen-specific antibody responses in the absence of other αβ T lymphocytes. We further previous work on MAIT-B cell help responses in animal models (*25*, *26*), by using an adoptive transfer model to show that MAIT cells are sufficient to increase functional anti-bacterial antibodies in the context of a mucosal challenge. Most notably, we show that adoptive transfer of MAIT cells rescues the deficiency in *V.c*-specific IgA and vibriocidal antibodies of infected TCRα$^{-/-}$ mice when compared to infected WT mice. Examination of antibody kinetics of *V.c* specific IgA in mice receiving MAIT transfer suggest a memory phenotype, based on substantial increases on Day 35 (one-week post re-challenge) (Fig. 6A), and is associated with higher lung PB/PC and memory B cell frequencies (Fig. 5F and G). Interestingly, we also report MAIT-*V.c* mice had significant systemic *V.c* specific IgA and total IgA responses compared to Sham-*V.c* mice (Fig. 6A and fig. S5A). These data may be a result of the mucosal nature of the intranasal challenge, which has shown

to induce both mucosal and systemic immunity in other bacterial infections (*78*). Notably, increases in total IgA in MAIT-PBS mice suggests MAITs may specifically promote IgA class switching. In support, pulmonary MAITs in mice have recently been shown to produce both IL-10 (*79*) and TGF1-β (*80*), key cytokines in IgA class switching (*81*). Although CXCR5 staining of lung MAITs suggests a similar Tfh-like MAIT phenotype in mice (Fig. 5C and D), limitations of available reagents for identifying murine MAITs by IHC precludes our ability to confirm a MAITfh subset in mice. Future analysis of lung and lymph node MAITs is necessary to confirm a MAITfh subset in mice and its potential role in IgA class switching and antibody production. Given that systemic *V. cholerae* specific IgA and vibriocidal responses strongly correlate with protection against subsequent cholera re-infection (*62*, *64*, *65*), these are promising data in the context of mucosal vaccines, where IgA is often the primary means of protection, and development of long-lasting protective memory responses is limiting (*82*).

In addition to promoting a protective antibody response, we report amplification of non-specific antibodies following MAIT transfer. We report similar *V. cholerae* lysate IgG (Fig. 6D) and IgM (fig. S5B), total IgA responses (fig. S5H), and similar changes in B cell subset frequencies in our MAIT-PBS and MAIT-*V.c* groups (Fig. 5E-H). Similar MAIT amplification of non-specific responses were reported in non-human primates (*26*) and FcγRIIB$^{-/-}$ mice (*25*). Specifically, Rahman et al. reported increased total IgM and IgG antibody production and increased IgD^{-} B cells (indicating class switching) when non-human primate MAITs were co-cultured with B cells. Murayama et. al 2019 show increases in total IgG and anti-dsDNA IgG and IgA when MAITs were co-cultured with B cells from FcγRIIB$^{-/-}$ mice. They also report reduction in anti-dsDNA IgG in MR1$^{-/-}$ (MAIT deficient) FcγRIIB$^{-/-}$ mice, though total IgG was not published. It should be noted that in all studies, MAITs were either activated *in vitro* in direct co-culture, or *in vivo* in the absence of regulatory T cells (TCRα$^{-/-}$ mice). Therefore, such responses may be a result of lack of either MAIT and/or B cell regulation leading to aberrant antibody responses. This has interesting consequences in the setting of mucosal immunity and in autoimmunity. In a setting of proper T

and B cell regulation, MAITs may help to promote anti-microbial responses and therefore could potentially be targeted as a vaccine adjuvant. Conversely, in a dysregulated environment, such as in FcγRIIB$^{-/-}$ or TCRα$^{-/-}$ mice, MAITs may enhance aberrant antibody production against self or commensal microbes thus enhancing the pro-inflammatory autoimmune state. These aberrant responses open many questions into cell extrinsic MAIT regulation which remains relatively unstudied.

There are a number of limitations that need to be addressed when considering the results of this study. In our human *in vitro* experiments, we compare PBMCs from healthy adults ages 18+ to tonsils from pediatric patients, ages 2-16, undergoing tonsillectomy. MAITs expand immediately after birth and reach adult frequencies by approximately 10 years of age, and most reach maturity (CD45RO^{+}) by 6 months of age (*83*). Therefore, it is possible that age may explain low MAIT percentage in tonsil samples, though we do not anticipate age-associated phenotypic effects. Secondly, the low sample size and lack of paired blood and tonsil samples significantly limits our TCR analyses (Fig. 4), and thus our observations regarding lack of differences in TCR usage between tonsil and blood MAITs, may be underpowered. Regarding our animal studies, a limitation of this study is the lack of mucosal antibody measurement as we recorded only systemic responses in serum. While mucosal secretory IgA (sIgA) and circulating IgA responses may differ, measurement of systemic antibodies is standard practice for mucosal vaccine response testing in humans, and *V.c* specific serum IgA response and vibriocidal titer strongly correlate with protection in humans (*62*, *64*, *65*). Thus, these serum responses are likely relevant to mucosal protection.

In conclusion, we identify a Tfh like MAIT population enriched near germinal centers of mucosal lymphoid tissues that express cytokine and transcriptional profiles consistent with B cell help. In addition, we show in an animal model that MAITs are sufficient to rescue pathogen-specific functional antibody responses following mucosal challenge in the absence of other classical T cells. Our work strengthens a growing body of evidence supporting the capacity of MAITs to aid in B cell help and antibody mediated

immunity, and support the expanding phenotypic heterogeneity of MAITs. As MAITs are enriched at the mucosa and can be activated with specific ligands, we hypothesize that they may be a promising target to enhance mucosal vaccines.

Materials and Methods

Peripheral blood and tonsil collection

Healthy adult blood was collected from residual leukocyte packs following blood donation (ARUP, Sandy, UT), and PBMC's were isolated by density gradient centrifugation (Lymphoprep, StemCell Technologies). Residual palatine tonsil samples were acquired from pediatric patients, ages 2-16, undergoing routine tonsillectomies for tonsillar hyperplasia or recurrent tonsillitis. All tonsil samples were stored on ice in complete media (RPMI 1640 with 10% FBS, 1% penicillin/streptomycin, and 15 mM HEPES) (R10) and processed within 2 hours of surgery. 1 cm x 1 cm pieces were cut and frozen in O.C.T. Compound (Fisher) at -80°C for later use. The remaining tonsil tissue was minced in media and dissociated using a 100 μM cell strainer. Tonsil mononuclear cells were isolated by density gradient centrifugation (Lymphoprep, StemCell Technologies). PBMC and tonsil mononuclear cells were frozen in media containing 25% FBS and 10% DMSO at -80°C for later use. All human samples were de-identified prior to receipt, and the research protocol was deemed exempt by the University of Utah Institutional Review Board (Protocol 100683).

Flow cytometry and cell sorting

Prior to surface staining, human and mouse single cell suspensions were labeled with Fixable Viability Dye eFluor 780 (eBioscience) according to manufacturer's protocol to delineate live cells. Cells were washed and incubated with fluorochrome conjugated antibodies for 20 min at room temperature (RT). Mouse cells were incubated in anti-mouse CD16/CD132 (Fc block) for 15 minutes prior to surface staining. Mouse and human MR1-Tetramers (NIH Tetramer Core) diluted 1:400 were added to surface stain. Prior to mouse MR1-Tetramer staining, cells were incubated for 15 minutes with unlabeled i6FP-Tetramer (NIH Tetramer Core) to minimize non-specific binding. For intracellular cytokine staining, cells were fixed and permeabilized using Foxp3/Transcription Factor Staining Buffer set (eBioscience) according to manufacturer's protocol and incubated with fluorochrome conjugated antibodies for 40 min

at RT. Cells were analyzed using BD LSR Fortessa for phenotypic analyses, or Aria II (BD Biosciences) for cell sorting. The following monoclonal antibodies to human were used : CD3- AF700 (clone OKT3), CD8-FITC/BV605 (cloneSK1, TCR Vα7.2-BV711/PE-Cy7 (clone 3C10), PD1-BV605/AF700 (clone EH12-2H7), ICOS-PerCP-Cy5.5/BV605 (clone C398.4A), CXCR5-PE-Cy7/APC (clone J252D4), IL-21-APC (clone 3A3-N2), IFNγ-BV421 (clone B27), IL-6-FitC (clone MQ2-13A5), IL-10-PerCP-Cy5.5 (clone JES2-9D7), CD161-AF488 (clone HP-3610) (Biolegend), CD4-BUV496 (clone SK3), CD3-BUV395 (clone SK7) (BD Biosciences). The following monoclonal antibodies to mouse were used: CD3-PE-Dazzle594 (clone 17A2), TCRβ-BV421 (clone H57-597), CXCR5-BV605 (clone L138D7), CD44-BV650 (clone IM7), TCRγδ-PE-Cy7 (clone GL3), CD8-APC (clone 53-6.7), CD45R-PE-Cy5 (clone RA3-6B2), IgD-BV510 (clone 11-26c.2a), CD138-BV605 (clone 281-2), CD38-PE-Cy7 (clone 90, CD27-APC (clone LG-3A10) (Biolegend), CD4-FITC (clone GK1.5) (Tonbo Biosciences).

In vitro stimulation assays

For flow cytometry intracellular cytokine staining, 1-2 x 10^6 mononuclear cells isolated from blood or tonsil samples were cultured in a round bottom 96 well plate at 37°C 5% CO_2 in R10 media for 6 hours with or without 200 ng/ml phorbol myristate acetate (PMA) and 1.0 μg/ml Ionomycin (Sigma-Aldrich). Brefeldin A Solution (Biolegend) was added at 1X for the final 4 hours. For measurement of IL-21 production, tonsil mononuclear cells were sorted into $CD8^+$ $CXCR5^-$, $CD4^+$ $CXCR5^+$ $PD1^{High}$, MR1-Tet^+, Vα7.2^+, $CXCR5^-$, MR1-Tet^+, Vα7.2^+, $CXCR5^+$ populations and $4x10^4$ cells in R10 media were cultured in a round bottom 96 well plate for 48 h with 20 ng/ml PMA and 1.0 μg/ml Ionomycin as described in Shen et al (*48*). Plates were centrifuged and cell supernatant was isolated for ELISAs.

qRT-PCR

PBMC and tonsil $CD8^+$ $CXCR5^-$, $CD4^+$ $CXCR5^+$, MR1-Tet^+ Vα7.2^+ $CXCR5^-$, MR1-Tet^+ Vα7.2^+ $CXCR5^+$ cells were sorted into TRIzol Reagent (Qiagen). Total RNA was isolated using the RNeasy

Micro kit and cDNA synthesized a High-Capacity cDNA Reverse Transcription Kit (Applied Biosystems). Targeted qPCR was performed using the QuantStudio 6 Real-Time PCR system using the following Taqman Primers (Applied Biosystems): BCL6 (Hs00153368_m1), Tnfsf13b (Hs00198106_m1), IL6 (Hs00174131_m1), IL10 (Hs00961622_m1), IL21 (Hs00222327_m1), TNFα (Hs00174128_m1), TGFB1 (HS00998133_m1), Tcf7 (Hs01556515_m1), Tbx21 (Hs00894392_m1), Runx3 (Hs01091094_m1), Rorc (Hs01076112_m1), Perforin (Hs00169473_m1), Pdcd1 (Hs01550088_m1), Il17a (Hs00174383_m1), Ifnγ (Hs00989291_m1), Icos (Hs00359999_m1), Gzmb (Hs00188051_m1, Cxcr5 (Hs00173527_m1), Cd40l (Hs00163934_m1), Cd38 (Hs01120071_m1), Blimp1 (Hs00153357_m1), Ascl2 (Hs00270888_s1), ActB (Hs99999903_m1).

ELISAs and Vibriocidal assay

IL-21 concentration from tonsil mono-cultures was measured using Human IL-21 ELISA MAX Deluxe kit (Biolegend) according to manufacturer's protocol. Serum *V.c* Lysate, OSP:BSA and CT ELISAs were performed as follows. Nunc Maxisorp flat bottom 96 well plates (Invitrogen) were coated with *V.c* Lysate or OSP:BSA (gift from Dr. Edward Ryan (Massachusetts General Hospital, Boston, MA) (1.0 μg/ml) in PBS and incubated overnight at 4°C. For CT ELISAs, Nunc plates were first coated with Monosialoganglioside G_{M1} (Sigma-Aldrich) (1.0 μg/ml) in 50mM carbonate buffer overnight at 4°C. Plates were subsequently blocked with 1% bovine serum albumin (BSA) (Sigma-Aldrich) and incubated overnight with CT (Sigma-Aldrich) (2.5 μg/ml) in carbonate buffer. All plates were then blocked with 1% BSA and 25 μl of mouse serum diluted 1:10 in 0.1% BSA-0.5% Tween 20 in PBS (BSA-PBST) was added for 2 hours. Plates were incubated with anti-mouse IgG (Invitrogen), IgA (Invitrogen), or IgM (Life Technologies) HRP conjugate diluted 1:1000 in BSA-PBST for 2 hours. 100 μl of TMB substrate (Thermo Fisher) was added and plates were immediately read kinetically at 405 nm (7 min x 1 min intervals) using plate reader (Biotek). ELISA measurements were recorded as max interval slope and normalized to pooled positive mouse sera included on each plate. Total Ig ELISAs were performed as

described above except Nunc plates were pre-coated with anti-mouse IgA (clone RMA1), anti-mouse IgG (clone Poly 4053), or anti-mouse IgM (clone RMM-1) (Biolegend) and standard curves were generated using 2-fold dilutions of purified Mouse IgA, IgM and IgG (Southern Biotech). Plates were incubated with corresponding anti-mouse HRP antibodies and TMB substrate was neutralized after 10 min with 0.2 N HCl. Plates were read at 605 nm and concentrations were calculated based on the standard curve. Vibriocidal titer was measured as described (*84*). *Vibrio cholerae* serotype 01 Strain El Tor Inaba N16961 grown in LB media was used as target organism for assay, and serum samples were diluted to a starting concentration of 1:5.

Immunofluorescence staining

Unfixed pediatric tonsil samples frozen in OCT medium were cut into 9μm thick sections using a cryostat (Leica) and stored at -80°C. Tonsil sections were brought to room temperature and then fixed at -20°C for 10 min in pre-cooled 50:50 Acetone:Methanol solution. Sections were dried and then rehydrated in PBS for 5 min with gentle shaking. The sections were then blocked in 2% normal mouse serum (Invitrogen) for 1 hour and subsequently stained overnight at 4°C with mouse anti-human TCR Vα7.2-PE (Clone 3C10, Biolegend), mouse anti-human CD161-AF488 (Clone NKR-P1A, Biolegend), mouse anti-human IgD-BV421 (Clone IA6-2, Biolegend) and mouse anti-human PD1-APC (Clone EH1202H7, Biolegend) all diluted 1:100. Sections were washed 3x in PBS and mounted using ProLong Gold Antifade Mounting media (Thermo Fisher). Full tonsil cross section images were acquired using the Leica Sp8 Confocal microscope and then processed and analyzed using ImageJ.

Single cell TCR sequencing

MAITs from PBMC's and tonsils were single cell sorted using the Aria II cell sorter (BD Biosciences) directly into One Step RT-PCR reaction mix (NEB) loaded in MicroAmp Optical 96-well reaction plates (Applied Biosystems). MAITs were defined as $CD3^+$ $V\alpha7.2^+$ MR1-Tetramer$^+$ cells. Following reverse

transcription and preamplification reaction, a series of three nested PCR's were run using primers for TCR sequence and gene expression as described (*57*). Subsequent sequencing data analysis was performed as described (*57*).

Bacterial culture and V. cholerae lysate preparation

The attenuated *Salmonella* Typhimurium strain BMM50 was a gift from Dr. Stephen McSorely (UC Davis, Davis, CA). BMM50, like previously published *S.* Typhimurium BRD509 (*39*), has a deleted *aroA* gene and intact riboflavin pathway. *Vibrio cholerae* serotype 01 Strain El Tor Inaba N16961 was a gift from Dr. Edward Ryan (Massachusetts General Hospital, Boston, MA). All strains were inoculated from single colonies into Luria Bertani (LB) broth shaking at 220 RPM 37°C overnight. They were then subcultured 1:10 in fresh LB and incubated for 3-4 hours shaking at 37°C until log phase was reached. Cultures were washed 2x in sterile PBS and normalized to 0.1 OD600 using a microplate absorbance spectrophotometer (BioRad). *V. cholerae* at 0.1 OD600 was used as inoculum for intranasal challenge model. *S.* Typhimurium BMM50 was diluted 1:10 with PBS to an OD600 of 0.01 for adoptive transfer inoculum. *V. cholerae* lysate for ELISAs was prepared as follows. *V. cholerae* was cultured from a single colony in LB broth shaking at 220 RPM 37°C overnight. *V. c* culture was then pelleted and washed 3x with cold sterile PBS. Following resuspension in PBS, sample was sonicated at 40% power 4 x 1 min intervals, keeping on ice for 1 minute between runs. Sonicated sample was then centrifuged at 15000 rpm x 10 min at 4°C, and the supernatant removed and sterilized using 0.2 μm syringe filter (Thermo Fisher). Protein content was measured using 260/280 absorbance ratio with Take3 Micro-Volume Plate reader (BioTek)

Mice

T*cra*^{tm1Mom}/J mice (*85*) (on a B6 background) were obtained from The Jackson Laboratory (Bar Harbor, ME) and bred at the University of Utah Comparative Medicine Center mouse facility. WT C57BL/6J

mice were obtained directly from The Jackson Laboratory prior to the start of the experiment. 6-10-week-old female and male mice were used in adoptive transfer studies. All mice were housed under specific pathogen-free conditions. Experiments were performed in strict accordance with the NIH guide for the Care and Use of Laboratory animals and institutional guidelines for animal care at the University of Utah under approved protocol #17-01011.

Adoptive transfer

Adoptive transfer of pulmonary MAITs was adapted from protocol described (*40*). C57BL/6 mice were infected i.n. with 10^6 CFU *S.* Typhimurium BMM50 suspended in 50 µl sterile PBS (25 µl per nares). Mice were rested for 7 days to allow for MAIT expansion, in which mice were weighed daily and evaluated for signs of clinical pneumonia symptoms (respiratory distress, inactivity, ruffled fur, hunched posture). Mice with loss of >20% of body weight and/or severe clinical symptoms were euthanized. On day 7, mice were euthanized and the lungs were perfused with 10 mls of PBS through the heart and then removed. Single cells suspensions of lungs were prepared using the gentleMacs Lung Dissociation kit, mouse (Miltenyi Biotech) according to the manufacturer's protocol. Red blood cells were lysed using ACK Lysis buffer (Thermo Fisher), and single cell suspensions were stained and sorted using the BD FACS Aria II. MAITs were defined as live $CD3^+$ $B220^-$ $TCR\gamma\delta^-$ $CD44^{high}$ $TCR\beta^+$ MR1-Tetramer$^+$ lymphocytes. Approximately $5x10^4$ - $1x10^5$ MAITs were sorted per mouse. 10^5 MAITs suspended in 100 µl was transferred via retroorbital injections into lightly anesthetized mice. Transferred mice were monitored to confirm recovery following injections, and rested for 2 weeks to allow for MAIT expansion before use in intranasal challenge model.

Intranasal challenge model

The following protocol was adapted from Nygren et al (*60*) to induce *V. cholerae* specific antibody responses through a prime-boost live bacterial model. In brief, on Day 0 mice were anesthetized using

isoflurane and infected i.n. with 10^6-10^7 CFU *V. cholerae* 01 Biotype El Tor Serotype Inaba suspended in 50 µl sterile PBS (25 µl per nares). Mice were monitored for 7 days post infection for weight loss and clinical signs of pneumoniae (outlined above). Mice with loss of >20% of body weight and/or severe clinical symptoms were euthanized. Mice were subsequently re-challenged on Day 28 using the above protocol. Blood samples were collected weekly, prior to infections on Day 0 and 28, from submandibular bleeds on lightly isoflurane anesthetized mice. Blood serum was isolated using BD Microtainer SST tubes (BD Biosciences) according to the manufacturer's protocol. On Day 42 (2 weeks post re-challenge), mice were euthanized using a bell jar and isoflurane. Blood was collected immediately via cardiac puncture and serum isolated. Lungs were perfused and single cell suspensions were processed as described above. Spleens were excised, ground through 70 µm filters in cold R10 media. Red blood cells were lysed using ACK Lysis Buffer (Thermo Fisher). 1-2x10^6 cells from lung and spleen cell suspensions were stained with fluorochrome conjugated antibodies for flow cytometric analyses.

Statistical analysis

All statistical tests were performed using Prism version 8.4.2 (GraphPad Software, La Jolla, CA, USA). Differences were compared using two-tailed Mann Whitney *U* tests, or Multiple t tests comparisons accounting for False Discoveries using the Benjamini, Krieger and Yekutieli correction as indicated. Graphs were created using Prism or R (Vienna, Austria) and the graphing package ggplot2 (H. Wickham, Springer-Verlag, NY, USA).

References

1. C. Gutzeit, G. Magri, A. Cerutti, Intestinal IgA production and its role in hot-microbe interaction. *Immunol. Rev.* **260**, 76–85 (2014).

2. O. Pabst, E. Slack, IgA and the intestinal microbiota: the importance of being specific. *Mucosal Immunol.* **13**, 12–21 (2020).

3. S. Hardtke, L. Ohl, R. Förster, Balanced expression of CXCR5 and CCR7 on follicular T helper cells determines their transient positioning to lymph node follicles and is essential for efficient B-cell help. *Blood.* **106**, 1924–1931 (2005).

4. H. Qi, T follicular helper cells in space-time. *Nat. Rev. Immunol.* **16**, 612–625 (2016).

5. J. Shi, S. Hou, Q. Fang, X. Liu, X. Liu, H. Qi, PD-1 Controls Follicular T Helper Cell Positioning and Function. *Immunity*. **49**, 264-274.e4 (2018).

6. A. Tafuri, A. Shahinian, F. Bladt, S. K. Yoshinaga, M. Jordana, A. Wakeham, L. M. Boucher, D. Bouchard, V. S. F. Chan, G. Duncan, B. Odermatt, A. Ho, A. Itie, T. Horan, J. S. Whoriskey, T. Pawson, J. M. Penninger, P. S. Ohashi, T. W. Mak, ICOS is essential for effective T-helper-cell responses. *Nature*. **409**, 105–109 (2001).

7. G. Van Kooten, J. Banchereau, CD40-CD40 ligand. *J. Leukoc. Biol.* **67**, 2–17 (2000).

8. K. Ozaki, R. Spolski, C. G. Feng, C. F. Qi, J. Cheng, A. Sher, H. C. Morse, C. Liu, P. L. Schwartzberg, W. J. Leonard, A critical role for IL-21 in regulating immunoglobulin production. *Science (80-.).* **298**, 1630–1634 (2002).

9. G. Galli, P. Pittoni, E. Tonti, C. Malzone, Y. Uematsu, M. Tortoli, D. Maione, G. Volpini, O. Finco, S. Nuti, S. Tavarini, P. Dellabona, R. Rappuoli, G. Casorati, S. Abrignani, Invariant NKT cells sustain specific B cell responses and memory. *Proc. Natl. Acad. Sci. U. S. A.* **104**, 3984–9 (2007).

10. E. Tonti, G. Galli, C. Malzone, S. Abrignani, G. Casorati, P. Dellabona, NKT-cell help to B lymphocytes can occur independently of cognate interaction. *Blood*. **113**, 370–376 (2009).

11. S. T. Scanlon, S. Y. Thomas, C. M. Ferreira, L. Bai, T. Krausz, P. B. Savage, A. Bendelac,

Airborne lipid antigens mobilize resident intravascular NKT cells to induce allergic airway inflammation. *J. Exp. Med.* **208**, 2113–2124 (2011).

12. E. A. Leadbetter, M. Brigl, P. Illarionov, N. Cohen, M. C. Luteran, S. Pillai, G. S. Besra, M. B. Brenner, NK T cells provide lipid antigen-specific cognate help for B cells. *Proc. Natl. Acad. Sci.* **105**, 8339–8344 (2008).

13. P. Barral, J. Eckl-Dorna, N. E. Harwood, C. De Santo, M. Salio, P. Illarionov, G. S. Besra, V. Cerundolo, F. D. Batista, B cell receptor-mediated uptake of CD1d-restricted antigen augments antibody responses by recruiting invariant NKT cell help in vivo. *Proc. Natl. Acad. Sci.* **105**, 8345–8350 (2008).

14. I. L. King, A. Fortier, M. Tighe, J. Dibble, G. F. M. Watts, N. Veerapen, A. M. Haberman, G. S. Besra, M. Mohrs, M. B. Brenner, E. A. Leadbetter, Invariant natural killer T cells direct B cell responses to cognate lipid antigen in an IL-21-dependent manner. *Nat. Immunol.* **13**, 44–50 (2012).

15. E. Tonti, M. Fedeli, A. Napolitano, M. Iannacone, U. H. von Andrian, L. G. Guidotti, S. Abrignani, G. Casorati, P. Dellabona, Follicular Helper NKT Cells Induce Limited B Cell Responses and Germinal Center Formation in the Absence of CD4 + T Cell Help . *J. Immunol.* **188**, 3217–3222 (2012).

16. H. B. Shah, S. K. Joshi, M. L. Lang, CD40L-null NKT cells provide B cell help for specific antibody responses. *Vaccine*. **29**, 9132–9136 (2011).

17. P. Rampuria, G. A. Lang, T. S. Devera, C. Gilmore, J. D. Ballard, M. L. Lang, Coordination between T helper cells, iNKT cells, and their follicular helper subsets in the humoral immune response against *Clostridium difficile* toxin B. *J. Leukoc. Biol.* **101**, 567–576 (2017).

18. P. P. Chang, P. Barral, J. Fitch, A. Pratama, C. S. Ma, A. Kallies, J. J. Hogan, V. Cerundolo, S. G. Tangye, R. Bittman, S. L. Nutt, R. Brink, D. I. Godfrey, F. D. Batista, C. G. Vinuesa, Identification of Bcl-6-dependent follicular helper NKT cells that provide cognate help for B cell responses. *Nat. Immunol.* **13**, 35–43 (2012).

19. N. Caccamo, L. Battistini, M. Bonneville, F. Poccia, J. J. Fournie, S. Meraviglia, G. Borsellino, R. A. Kroczek, C. La Mendola, E. Scotet, F. Dieli, A. Salerno, CXCR5 Identifies a Subset of V 9V 2 T Cells which Secrete IL-4 and IL-10 and Help B Cells for Antibody Production. *J. Immunol.* **177**, 5290–5295 (2006).

20. R. R. Bansal, C. R. Mackay, B. Moser, M. Eberl, IL-21 enhances the potential of human γδ T cells to provide B-cell help. *Eur. J. Immunol.* **42**, 110–119 (2012).

21. R. M. Rezende, A. J. Lanser, S. Rubino, C. Kuhn, N. Skillin, T. G. Moreira, S. Liu, G. Gabriely, B. A. David, G. B. Menezes, H. L. Weiner, γδ T cells control humoral immune response by inducing T follicular helper cell differentiation. *Nat. Commun.* **9** (2018), doi:10.1038/s41467-018-05487-9.

22. D. T. Leung, T. R. Bhuiyan, N. S. Nishat, M. R. Hoq, A. Aktar, M. A. Rahman, T. Uddin, A. I. Khan, F. Chowdhury, R. C. Charles, J. B. Harris, S. B. Calderwood, F. Qadri, E. T. Ryan, Circulating mucosal associated invariant T cells are activated in Vibrio cholerae O1 infection and associated with lipopolysaccharide antibody responses. *PLoS Negl. Trop. Dis.* **8**, e3076 (2014).

23. M. S. Bennett, S. Trivedi, A. S. Iyer, J. S. Hale, D. T. Leung, Human mucosal-associated invariant T (MAIT) cells possess capacity for B-cell help. *J. Leukoc. Biol.* **102**, 1261–1269 (2017).

24. J. Jiang, Z. Cao, PD-1-expressing MAIT cells from patients with tuberculosis exhibit elevated production of CXCL13, 1–15 (2020).

25. G. Murayama, A. Chiba, H. Suzuki, A. Nomura, T. Mizuno, T. Kuga, S. Nakamura, H. Amano, S. Hirose, K. Yamaji, Y. Suzuki, N. Tamura, S. Miyake, A Critical Role for Mucosal-Associated Invariant T Cells as Regulators and Therapeutic Targets in Systemic Lupus Erythematosus. *Front. Immunol.* **10**, 2681 (2019).

26. M. A. Rahman, E. Ko, F. Bhuyan, G. Enyindah-asonye, R. Hunegnaw, S. H. Hait, C. J. Hogge, D. J. Venzon, T. Hoang, M. Robert-guroff, Mucosal-associated invariant T (MAIT) cells provide B-cell help in vaccinated and subsequently SIV- infected Rhesus Macaques. *Sci. Rep.*, 1–17 (2020).

27. F. Tilloy, E. Treiner, S. H. Park, C. Garcia, F. Lemonnier, H. de la Salle, A. Bendelac, M.

Bonneville, O. Lantz, An invariant T cell receptor alpha chain defines a novel TAP-independent major histocompatibility complex class Ib-restricted alpha/beta T cell subpopulation in mammals. *J. Exp. Med.* **189**, 1907–21 (1999).

28. R. Reantragoon, A. J. Corbett, I. G. Sakala, N. A. Gherardin, J. B. Furness, Z. Chen, S. B. G. Eckle, A. P. Uldrich, R. W. Birkinshaw, O. Patel, L. Kostenko, B. Meehan, K. Kedzierska, L. Liu, D. P. Fairlie, T. H. Hansen, D. I. Godfrey, J. Rossjohn, J. McCluskey, L. Kjer-Nielsen, Antigen-loaded MR1 tetramers define T cell receptor heterogeneity in mucosal-associated invariant T cells. *J. Exp. Med.* **210**, 2305–20 (2013).

29. M. Lepore, A. Kalinicenko, A. Colone, B. Paleja, A. Singhal, A. Tschumi, B. Lee, M. Poidinger, F. Zolezzi, L. Quagliata, P. Sander, E. Newell, A. Bertoletti, L. Terracciano, G. De Libero, L. Mori, Parallel T-cell cloning and deep sequencing of human MAIT cells reveal stable oligoclonal TCRβ 2 repertoire. *Nat. Commun.* **5** (2014), doi:10.1038/ncomms4866.

30. E. Martin, E. Treiner, L. Duban, L. Guerri, H. Laude, C. Toly, V. Premel, A. Devys, I. C. Moura, F. Tilloy, S. Cherif, G. Vera, S. Latour, C. Soudais, O. Lantz, Stepwise Development of MAIT Cells in Mouse and Human. *PLoS Biol.* **7**, e1000054 (2009).

31. L. Le Bourhis, E. Martin, I. Péguillet, A. Guihot, N. Froux, M. Coré, E. Lévy, M. Dusseaux, V. Meyssonnier, V. Premel, C. Ngo, B. Riteau, L. Duban, D. Robert, M. Rottman, C. Soudais, O. Lantz, Antimicrobial activity of mucosal-associated invariant T cells. *Nat. Immunol.* **11**, 701–708 (2010).

32. M. Dusseaux, E. Martin, N. Serriari, I. Péguillet, V. Premel, D. Louis, M. Milder, L. Le Bourhis, C. Soudais, E. Treiner, O. Lantz, Human MAIT cells are xenobiotic-resistant, tissue-targeted, CD161 hi IL-17-secreting T cells. *Blood*. **117**, 1250–1259 (2011).

33. A. Rahimpour, H. F. Koay, A. Enders, R. Clanchy, S. B. G. Eckle, B. Meehan, Z. Chen, B. Whittle, L. Liu, D. P. Fairlie, C. C. Goodnow, J. McCluskey, J. Rossjohn, A. P. Uldrich, D. G. Pellicci, D. I. Godfrey, Identification of phenotypically and functionally heterogeneous mouse mucosal-associated invariant T cells using MR1 tetramers. *J. Exp. Med.* **212**, 1095–1108 (2015).

34. A. Kurioka, J. E. Ussher, C. Cosgrove, C. Clough, J. R. Fergusson, K. Smith, Y. H. Kang, L. J. Walker, T. H. Hansen, C. B. Willberg, P. Klenerman, MAIT cells are licensed through granzyme exchange to kill bacterially sensitized targets. *Mucosal Immunol.* **8**, 429–440 (2015).

35. L. Le Bourhis, M. Dusseaux, A. Bohineust, S. Bessoles, E. Martin, V. Premel, M. Coré, D. Sleurs, N. E. Serriari, E. Treiner, C. Hivroz, P. Sansonetti, M. L. Gougeon, C. Soudais, O. Lantz, MAIT Cells Detect and Efficiently Lyse Bacterially-Infected Epithelial Cells. *PLoS Pathog.* **9** (2013), doi:10.1371/journal.ppat.1003681.

36. J. Dias, E. Leeansyah, J. K. Sandberg, Multiple layers of heterogeneity and subset diversity in human MAIT cell responses to distinct microorganisms and to innate cytokines. *Proc. Natl. Acad. Sci.* **114**, E5434–E5443 (2017).

37. A. Meierovics, W.-J. C. Yankelevich, S. C. Cowley, MAIT cells are critical for optimal mucosal immune responses during in vivo pulmonary bacterial infection. *Proc. Natl. Acad. Sci.* **110**, E3119–E3128 (2013).

38. P. Georgel, M. Radosavljevic, C. Macquin, S. Bahram, The non-conventional MHC class I MR1 molecule controls infection by Klebsiella pneumoniae in mice. *Mol. Immunol.* **48**, 769–775 (2011).

39. Z. Chen, H. Wang, C. D'Souza, S. Sun, L. Kostenko, S. B. G. Eckle, B. S. Meehan, D. C. Jackson, R. A. Strugnell, H. Cao, N. Wang, D. P. Fairlie, L. Liu, D. I. Godfrey, J. Rossjohn, J. McCluskey, A. J. Corbett, Mucosal-associated invariant T-cell activation and accumulation after in vivo infection depends on microbial riboflavin synthesis and co-stimulatory signals. *Mucosal Immunol.* **10**, 58–68 (2017).

40. H. Wang, C. D'Souza, X. Y. Lim, L. Kostenko, T. J. Pediongco, S. B. G. Eckle, B. S. Meehan, M. Shi, N. Wang, S. Li, L. Liu, J. Y. W. Mak, D. P. Fairlie, Y. Iwakura, J. M. Gunnersen, A. W. Stent, D. I. Godfrey, J. Rossjohn, G. P. Westall, L. Kjer-Nielsen, R. A. Strugnell, J. McCluskey, A. J. Corbett, T. S. C. Hinks, Z. Chen, MAIT cells protect against pulmonary Legionella longbeachae infection. *Nat. Commun.* **9**, 3350 (2018).

41. F. J. Radcliff, S. Waldvogel-thurlow, F. Clow, M. Mahadevan, J. Johnston, G. Li, T. Proft, R. G. Douglas, J. D. Fraser, Impact of Superantigen-Producing Bacteria on T Cells from Tonsillar Hyperplasia. *Pathogens*. **8**, 1–17 (2019).

42. E. Leeansyah, L. Loh, D. F. Nixon, J. K. Sandberg, Acquisition of innate-like microbial reactivity in mucosal tissues during human fetal MAIT-cell development. *Nat. Commun.* **5**, 1–10 (2014).

43. K. Franciszkiewicz, M. Salou, F. Legoux, Q. Zhou, Y. Cui, S. Bessoles, O. Lantz, MHC class I-related molecule, MR1, and mucosal-associated invariant T cells. *Immunol. Rev.* **272**, 120–138 (2016).

44. M. I. Vazquez, J. Catalan-Dibene, A. Zlotnik, B cells responses and cytokine production are regulated by their immune microenvironment. *Cytokine*. **74**, 318–326 (2015).

45. A. G. Zaretsky, J. J. Taylor, I. L. King, F. A. Marshall, M. Mohrs, E. J. Pearce, T follicular helper cells differentiate from Th2 cells in response to helminth antigens. *J. Exp. Med.* **206**, 991–999 (2009).

46. D. Fang, K. Cui, K. Mao, G. Hu, R. Li, M. Zheng, N. Riteau, S. L. Reiner, A. Sher, K. Zhao, J. Zhu, Transient T-bet expression functionally specifies a distinct T follicular helper subset. *J. Exp. Med.* **215**, 2705–2714 (2018).

47. P. Wang, Y. Wang, L. Xie, M. Xiao, J. Wu, L. Xu, Q. Bai, Y. Hao, Q. Huang, X. Chen, R. He, B. Li, S. Yang, Y. Chen, Y. Wu, L. Ye, The transcription factor T-bet is required for optimal type I follicular helper T cell maintenance during acute viral infection. *Front. Immunol.* **10**, 1–17 (2019).

48. J. Shen, X. Luo, Q. Wu, J. Huang, G. Xiao, L. Wang, B. Yang, H. Li, C. Wu, A subset of CXCR5+CD8+ T cells in the germinal centers from human tonsils and lymph nodes help B cells produce immunoglobulins. *Front. Immunol.* **9**, 1–12 (2018).

49. T. Leng, H. D. Akther, C. P. Hackstein, K. Powell, T. King, M. Friedrich, Z. Christoforidou, S. McCuaig, M. Neyazi, C. V. Arancibia-Cárcamo, J. Hagel, F. Powrie, R. S. Peres, V. Millar, D. Ebner, R. Lamichhane, J. Ussher, T. S. C. Hinks, E. Marchi, C. Willberg, P. Klenerman, TCR and Inflammatory Signals Tune Human MAIT Cells to Exert Specific Tissue Repair and Effector

Functions. *Cell Rep.* **28**, 3077-3091.e5 (2019).

50. M. Lettau, A. Wiedemann, E. V. Schrezenmeier, C. Giesecke-Thiel, T. Dörner, Human CD27+ memory B cells colonize a superficial follicular zone in the palatine tonsils with similarities to the spleen. A multicolor immunofluorescence study of lymphoid tissue. *PLoS One*. **15**, 1–17 (2020).

51. J. J. Hong, P. K. Amancha, K. Rogers, A. A. Ansari, F. Villinger, Spatial Alterations between CD4 + T Follicular Helper, B, and CD8 + T Cells during Simian Immunodeficiency Virus Infection: T/B Cell Homeostasis, Activation, and Potential Mechanism for Viral Escape . *J. Immunol.* **188**, 3247–3256 (2012).

52. G. Narayanan, J. E. McLaren, E. W. Meermeier, K. Ladell, G. M. Swarbrick, D. A. Price, T. G. Jessica, A. H. Worley, T. Vogt, E. B. Wong, D. M. Lewinsohn, The MAIT TCRβ chain contributes to discrimination of microbial ligand. *Immunol. Cell Biol.* (2020), doi:10.1111/imcb.12370.

53. L. J. Howson, G. Napolitani, D. Shepherd, H. Ghadbane, P. Kurupati, L. Preciado-Llanes, M. Rei, H. C. Dobinson, M. M. Gibani, K. W. W. Teng, E. W. Newell, N. Veerapen, G. S. Besra, A. J. Pollard, V. Cerundolo, MAIT cell clonal expansion and TCR repertoire shaping in human volunteers challenged with Salmonella Paratyphi A. *Nat. Commun.* **9**, 1–11 (2018).

54. V. Voillet, M. Buggert, C. K. Slichter, J. D. Berkson, F. Mair, M. M. Addison, Y. Dori, G. Nadolski, M. G. Itkin, R. Gottardo, M. R. Betts, M. Prlic, Human MAIT cells exit peripheral tissues and recirculate via lymph in steady state conditions. *JCI insight*. **3**, 1–10 (2018).

55. E. B. Wong, M. C. Gold, E. W. Meermeier, B. Z. Xulu, S. Khuzwayo, Z. A. Sullivan, E. Mahyari, Z. Rogers, H. Kløverpris, P. K. Sharma, A. H. Worley, U. Lalloo, P. Baijnath, A. Ambaram, L. Naidoo, M. Suleman, R. Madansein, J. E. McLaren, K. Ladell, K. L. Miners, D. A. Price, S. M. Behar, M. Nielsen, V. O. Kasprowicz, A. Leslie, W. R. Bishai, T. Ndung'u, D. M. Lewinsohn, TRAV1-2+ CD8+ T-cells including oligoconal expansions of MAIT cells are enriched in the airways in human tuberculosis. *Commun. Biol.* **2** (2019), doi:10.1038/s42003-019-0442-2.

56. L. Loh, N. A. Gherardin, S. Sant, J. C. Crawford, N. L. Bird, C. E. Van De Sandt, M. L. Moreira,

E. K. Allen, J. Crowe, T. Loudovaris, K. L. Flanagan, K. M. Quinn, J. Rossjohn, G. Paul, S. B. G. Eckle, J. Mccluskey, I. Dale, K. Kedzierska, J. C. Crawford, N. L. Bird, H. Koay, C. E. Van De Sandt, M. L. Moreira, M. Lappas, E. K. Allen, J. Crowe, T. Loudovaris, K. L. Flanagan, K. M. Quinn, J. Rossjohn, P. G. Thomas, Human Mucosal-Associated Invariant T Cells in Older Individuals Display Expanded TCR α β Clonotypes with Potent Antimicrobial Responses (2020), doi:10.4049/jimmunol.1900774.

57. A. Han, J. Glanville, L. Hansmann, M. M. Davis, Linking T-cell receptor sequence to functional phenotype at the single-cell level. *Nat. Biotechnol.* **32**, 684–692 (2014).

58. M. C. Gold, J. E. McLaren, J. A. Reistetter, S. Smyk-Pearson, K. Ladell, G. M. Swarbrick, Y. Y. L. Yu, T. H. Hansen, O. Lund, M. Nielsen, B. Gerritsen, C. Kesmir, J. J. Miles, D. A. Lewinsohn, D. A. Price, D. M. Lewinsohn, MR1-restricted MAIT cells display ligand discrimination and pathogen selectivity through distinct T cell receptor usage. *J. Exp. Med.* **211**, 1601–1610 (2014).

59. J. A. Kotov, M. K. Jenkins, Cutting Edge: T Cell–Dependent Plasmablasts Form in the Absence of Single Differentiated CD4 $^{+}$ T Cell Subsets. *J. Immunol.*, ji1801349 (2018).

60. E. Nygren, J. Holmgren, S. R. Attridge, Murine antibody responses following systemic or mucosal immunization with viable or inactivated Vibrio cholerae. *Vaccine*. **26**, 6784–6790 (2008).

61. D. J. Haney, M. D. Lock, J. K. Simon, J. Harris, M. Gurwith, Antibody-based correlates of protection against cholera: Analysis of a challenge study of a cholera-naive population. *Clin. Vaccine Immunol.* **24**, 1–11 (2017).

62. J. B. Harris, R. C. LaRocque, F. Chowdhury, A. I. Khan, T. Logvinenko, A. S. G. Faruque, E. T. Ryan, F. Qadri, S. B. Calderwood, Susceptibility to Vibrio cholerae infection in a cohort of household contacts of patients with cholera in Bangladesh. *PLoS Negl. Trop. Dis.* **2** (2008), doi:10.1371/journal.pntd.0000221.

63. R. Finkelstein, Vibriocidal Antibody Inhibition (VAI) Analysis: A Technique for the Identification of the Predominant Vibriocidal Antibodies in Serum and for the Detection and Identification of Vibrio Cholerae Antigens. *J. Immunol.* **89**, 264–271 (1962).

64. R. I. Glass, A. M. Svennerholm, M. R. Khan, S. Huda, M. Imdadul Huq, J. Holmgren, Seroepidemiological studies of EI tor cholera in bangladesh: Association of serum antibody levels with protection. *J. Infect. Dis.* **151**, 236–242 (1985).

65. A. S. Azman, J. Lessler, F. J. Luquero, T. R. Bhuiyan, A. I. Khan, F. Chowdhury, A. Kabir, M. Gurwith, A. A. Weil, J. B. Harris, S. B. Calderwood, E. T. Ryan, F. Qadri, D. T. Leung, Estimating cholera incidence with cross-sectional serology. *Sci. Transl. Med.* **11**, 1–11 (2019).

66. D. T. Leung, T. Uddin, P. Xu, A. Aktar, R. A. Johnson, M. A. Rahman, M. M. Alam, M. K. Bufano, G. Eckhoff, Y. Wu-Freeman, Y. Yu, T. Sultana, F. Khanam, A. Saha, F. Chowdhury, A. I. Khan, R. C. Charles, R. C. LaRocque, J. B. Harris, S. B. Calderwood, P. Kováč, F. Qadri, E. T. Ryan, Immune responses to the O-specific polysaccharide antigen in children who received a killed oral cholera vaccine compared to responses following natural cholera infection in Bangladesh. *Clin. Vaccine Immunol.* **20**, 780–788 (2013).

67. S. M. Patel, M. A. Rahman, M. Mohasin, M. A. Riyadh, D. T. Leung, M. M. Alam, F. Chowdhury, A. I. Khan, A. A. Weil, A. Aktar, M. Nazim, R. C. LaRocque, E. T. Ryan, S. B. Calderwood, F. Qadri, J. B. Harris, Memory B Cell Responses to Vibrio cholerae O1 Lipopolysaccharide Are Associated with Protection against Infection from Household Contacts of Patients with Cholera in Bangladesh. *Clin. Vaccine Immunol.* **19**, 842–848 (2012).

68. A. S. Iyer, A. S. Azman, M. Bouhenia, L. O. Deng, C. P. Anderson, M. Graves, P. Kováč, P. Xu, E. T. Ryan, J. B. Harris, D. A. Sack, F. J. Luquero, D. T. Leung, Dried Blood Spots for Measuring Vibrio cholerae-specific Immune Responses. *PLoS Negl. Trop. Dis.* **12** (2018), doi:10.1371/journal.pntd.0006196.

69. R. C. Kauffman, T. R. Bhuiyan, R. Nakajima, L. M. Mayo-Smith, R. Rashu, M. R. Hoq, F. Chowdhury, A. I. Khan, A. Rahman, S. K. Bhaumik, L. Harris, J. T. O'Neal, J. F. Trost, N. H. Alam, A. Jasinskas, E. Dotsey, M. Kelly, R. C. Charles, P. Xu, P. Kováč, S. B. Calderwood, E. T. Ryan, P. L. Felgner, F. Qadri, J. Wrammert, J. B. Harris, Single-cell analysis of the plasmablast response to Vibrio cholerae demonstrates expansion of cross-reactive memory B cells. *MBio.* **7**, 1–

11 (2016).

70. N. Rout, Enhanced Th1/Th17 Functions of CD161+ CD8+ T Cells in Mucosal Tissues of Rhesus Macaques. *PLoS One*. **11**, e0157407 (2016).

71. S. Crotty, T Follicular Helper Cell Differentiation, Function, and Roles in Disease. *Immunity*. **41**, 529–542 (2014).

72. M. Salio, O. Gasser, C. Gonzalez-Lopez, A. Martens, N. Veerapen, U. Gileadi, J. G. Verter, G. Napolitani, R. Anderson, G. Painter, G. S. Besra, I. F. Hermans, V. Cerundolo, Activation of Human Mucosal-Associated Invariant T Cells Induces CD40L-Dependent Maturation of Monocyte-Derived and Primary Dendritic Cells. *J. Immunol.*, ji1700615 (2017).

73. R. J. Johnston, A. C. Poholek, D. DiToro, I. Yusuf, D. Eto, B. Barnett, A. L. Dent, J. Craft, S. Crotty, Bcl6 and Blimp-1 are reciprocal and antagonistic regulators of T follicular helper cell differentiation. *Science (80-.).* **325**, 1006–1010 (2009).

74. R. Ettinger, S. Kuchen, P. E. Lipsky, The role of IL-21 in regulating B-cell function in health and disease. *Immunol. Rev.* **223**, 60–86 (2008).

75. D. Eto, C. Lao, D. DiToro, B. Barnett, T. C. Escobar, R. Kageyama, I. Yusuf, S. Crotty, IL-21 and IL-6 are critical for different aspects of B cell immunity and redundantly induce optimal follicular helper CD4 T cell (Tfh) differentiation. *PLoS One*. **6**, e17739 (2011).

76. L. Moens, S. G. Tangye, Cytokine-mediated regulation of plasma cell generation: IL-21 takes center stage. *Front. Immunol.* **5**, 1–13 (2014).

77. A. Cerutti, M. Cols, I. Puga, Activation of B cells by non-canonical helper signals. *EMBO Rep.* **13**, 798–810 (2012).

78. X. Shen, T. Lagergard, Y. Yang, M. Lindblad, M. Fredriksson, J. Holmgren, Systemic and mucosal immune responses in mice after mucosal immunization with group B streptococcus type III capsular polysaccharide-cholera toxin B subunit conjugate vaccine. *Infect. Immun.* **68**, 5749–5755 (2000).

79. H. Yu, A. Yang, S. Derrick, J. Y. W. Mak, L. Liu, D. P. Fairlie, S. Cowley, Artificially induced

MAIT cells inhibit M . bovis BCG but not M . tuberculosis during in vivo pulmonary infection. *Sci. Rep.*, 1–12 (2020).

80. S. Sakai, K. D. Kauffman, S. Oh, C. E. Nelson, C. E. B. Iii, D. L. Barber, MAIT cell-directed therapy of Mycobacterium tuberculosis infection. *Mucosal Immunol.*, 1–10 (2020).

81. A. Cerutti, The regulation of IgA class switching. *Nat. Rev. Immunol.* **8**, 421–434 (2008).

82. J. Holmgren, A. M. Svennerholm, Vaccines against mucosal infections. *Curr. Opin. Immunol.* **24**, 343–353 (2012).

83. G. Ben Youssef, M. Tourret, M. Salou, L. Ghazarian, V. Houdouin, S. Mondot, Y. Mburu, M. Lambert, S. Azarnoush, J.-S. Diana, A.-L. Virlouvet, M. Peuchmaur, T. Schmitz, J.-H. Dalle, O. Lantz, V. Biran, S. Caillat-Zucman, Ontogeny of human mucosal-associated invariant T cells and related T cell subsets. *J. Exp. Med.* **215**, 459–479 (2018).

84. F. Qadri, G. Mohi, J. Hossain, T. Azim, A. M. Khan, M. A. Salam, R. B. Sack, M. J. Albert, A. M. Svennerholm, Comparison of the vibriocidal antibody response in cholera due to Vibrio cholerae O139 Bengal with the response in cholera due to Vibrio cholerae O1. *Clin. Diagn. Lab. Immunol.* **2**, 685–8 (1995).

85. P. Mombaerts, A. R. Clarke, M. A. Rudnicki, J. Iacomini, S. Itohara, J. J. Lafaille, L. Wang, Y. Ichikawa, R. Jaenisch, M. L. Hooper, S. Tonegawa, Mutations in T-cell antigen receptor genes α and β block thymocyte development at different stages. *Nature*. **360**, 225–231 (1992).

Acknowledgements

Funding: This research was supported by the National Institutes of Health (R01 AI130378 to D.T.L. and T32 AI138945 to O.J.). This work was also supported by the University of Utah Flow Cytometry Facility in addition to the National Cancer Institute through Award Number P30CA042014. We would also like to thank the staff of the Office of Comparative Medicine, and University of Utah Cell Imaging Core.

Author Contributions: O.J. and D.T.L. designed and directed the project. O.J and S.T. performed the experiments. K.F. and J.S.H. contributed to experimental methodology. J.D.M. provided samples and resources. D.T.L acquired funding. O.J. and D.T.L wrote the paper, and all authors discussed results, provided critical feedback, and contributed to the final manuscript.

Declaration of interests: None.

Supplementary Materials

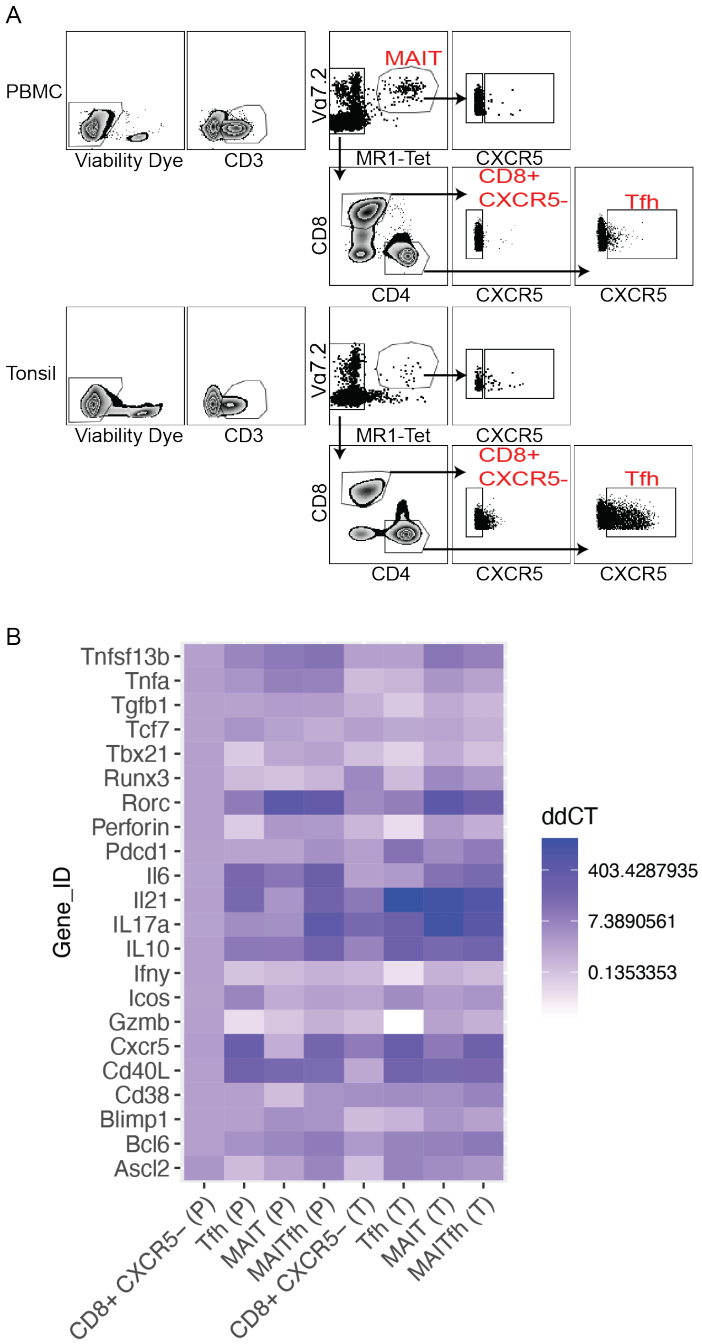

Supplementary Fig. 1. qPCR and flow gating strategy (Fig 2) and additional FAC sorted qPCR targets. Representative flow cytometry gating strategy for qPCR FAC sorted and flow populations in Fig.2 from (**A**) PBMC and (**B**) tonsils. (**C**) Heat map of additional qPCR targets described in Fig 2A-E. As described, data are represented as ΔΔCt relative to β-Actin and then the PBMC-CD8$^-$CXCR5$^-$ population. Rows denote gene ID and columns denote sample group (P=PBMC, T=tonsil). Heat map data are represented by mean of n=4 samples per group.

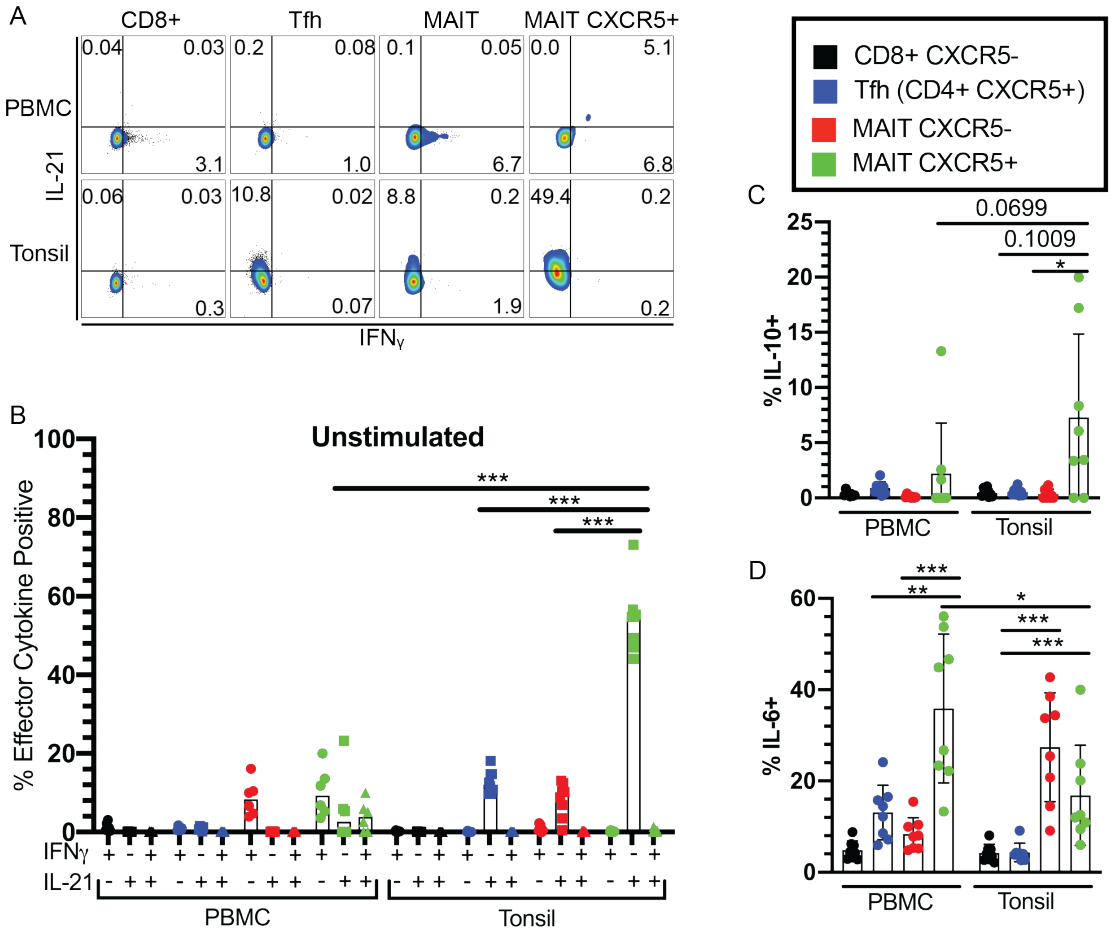

Supplementary Fig. 2. High IL-21 baseline expression in unstimulated CXCR5$^+$ MAITs in tonsils. (**A**) Representative flow cytometry from 6 hour no stimulation controls for PBMC and tonsil T cell populations showing IL-21 and IFNγ co-expression. (**B**) Frequency of T cell populations expressing IL-21, IFNγ or both. Data are represented median from two independent experiments. n≥5. Flow cytometry data showing frequency of T cell subsets expressing IL-10 (**C**) and IL-6 (**D**) following *in vitro* stimulation with 6 h PMA/Ionomycin. Data are represented as mean with SEM from 2 independent experiments. n=8. *$p < 0.05$, **$p<0.01$, ***$p<0.001$, ****$p<0.0001$ by two-tailed Mann-Whitney *U* test. Legend in black box denotes experimental groups.

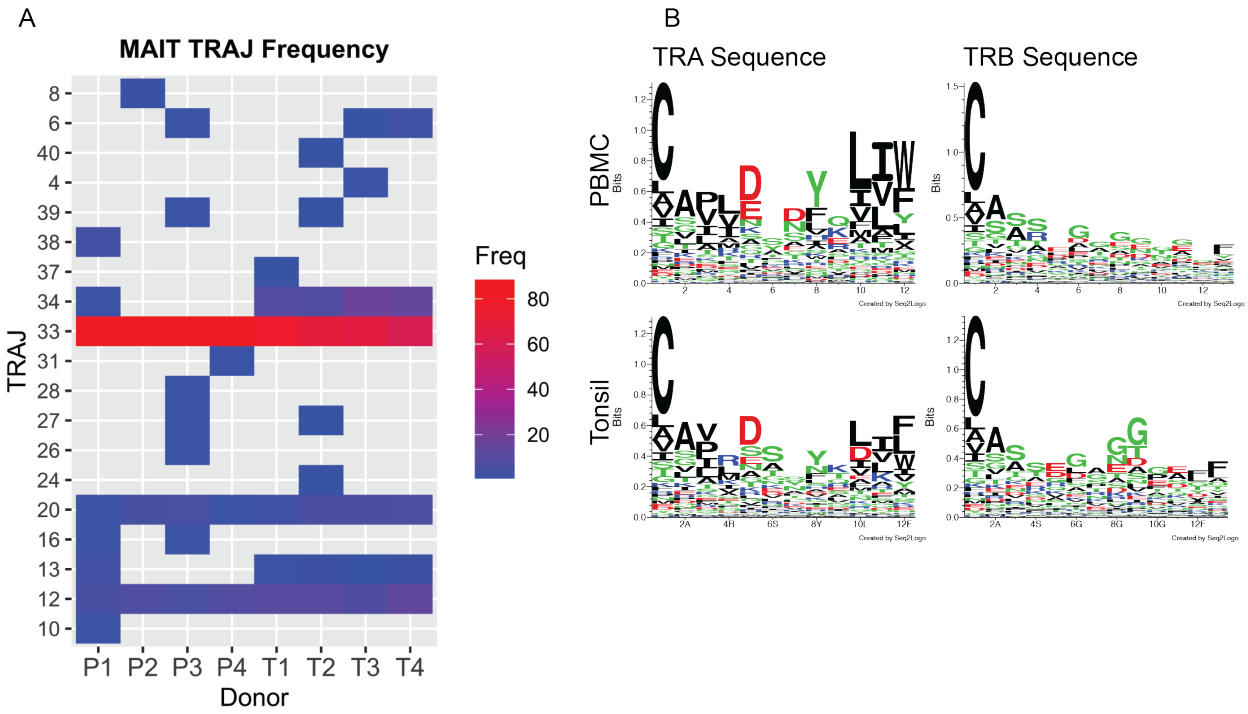

Supplementary Fig. 3. PBMC and tonsil MAIT TRAJ usage frequency and TRA-TRB Seq2logo plots.

(**A**) Heat map of TRAJ usage percent frequencies based on Illumina single cell TCR-Phenotype sequencing in tonsil and PBMC MAITs. Each column represents an individual donor (n=4). No statistical significance was found between tonsil and PBMC groups using Multiple t tests comparison accounting for False Discoveries using the Benjamini, Krieger and Yekutieli method. (**B**) Visual depiction of consensus CDR3α (left) and CDR3β (right) amino acid sequences from PBMC (top) and tonsil (bottom) MAITs. Analysis was confined to first 12 and 13 amino acids for CDR3α and CDR3β, respectively.

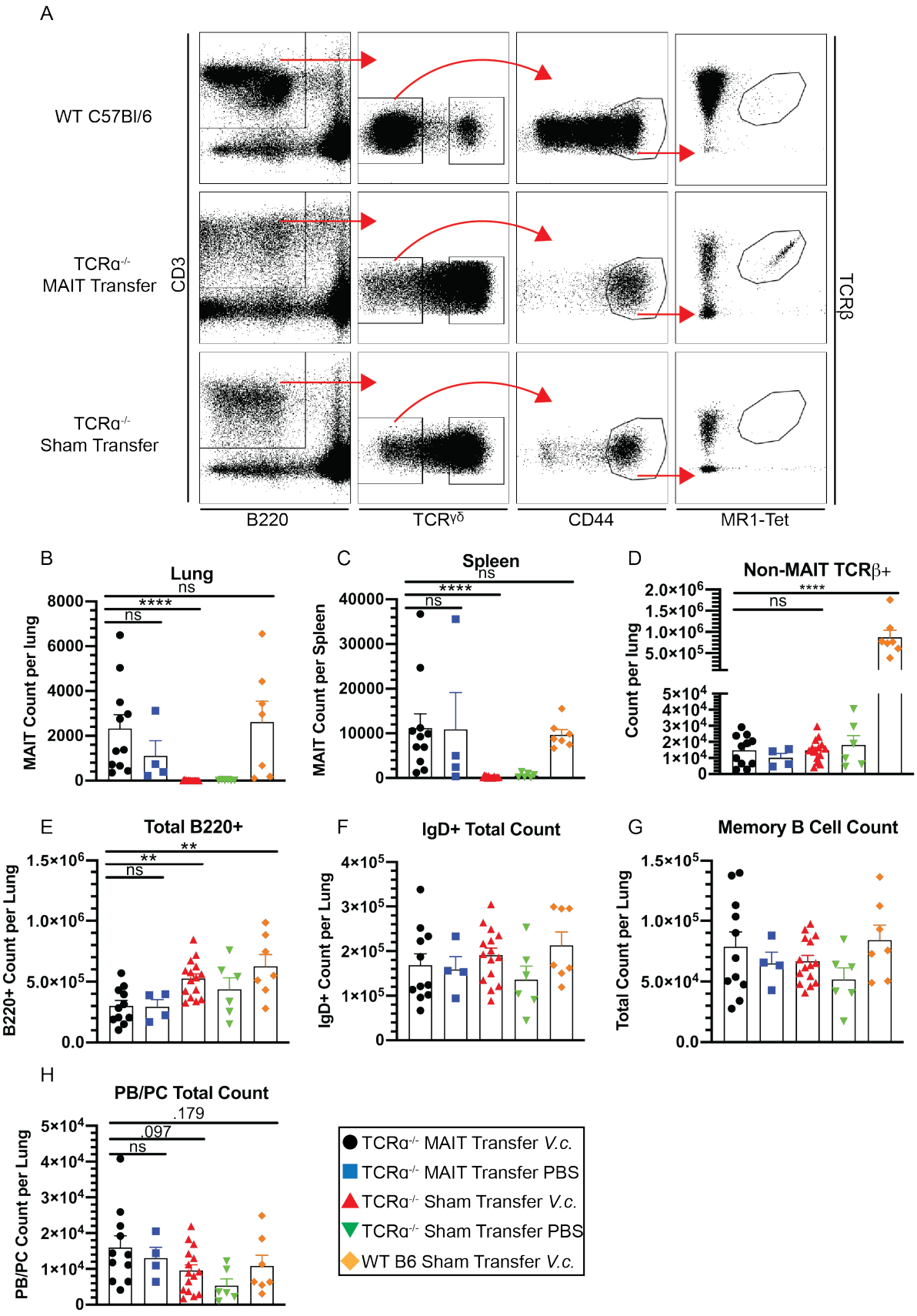

Supplementary Fig. 4. Flow gating for murine lung MAITs and B and T lymphocyte counts. (**A**) Representative flow gating of murine MAITs from digested lung tissue highlighted in Fig. 5a. MAITs were defined as live B220^{-} CD3^{+} TCRγδ^{-} CD44^{High} TCRβ^{+}MR1-Tetramer^{+}. Only WT-*V.c.*, MAIT-*V.c.*, and Sham-*V.c.* groups are portrayed. (**B**) Total MAIT count per lung. (**C**) Total MAIT cell count per spleen. (D) Total non-MAIT CD3^{+}TCRβ^{+}T cells per lung. (**E**) Total B220^{+} B cells per lung. (**F**) Total IgD^{+}Naïve B cells per lung. (**G**) Total IgD^{-} CD27^{+} CD38^{+} CD138^{-} Memory B cells per lung. (**H**) Total IgD^{-} CD27^{+} CD38^{+} CD138^{++} PB/PCs per lung. Data are represented as Mean with SEM from 4 independent experiments. n= 4-15 mice per group. $*p < 0.05$, $**p<0.01$, $***p<0.001$, $****p<0.0001$ by two-tailed Mann-Whitney *U* test. by two-tailed Mann-Whitney *U* test. Legend in black box denotes experimental groups.

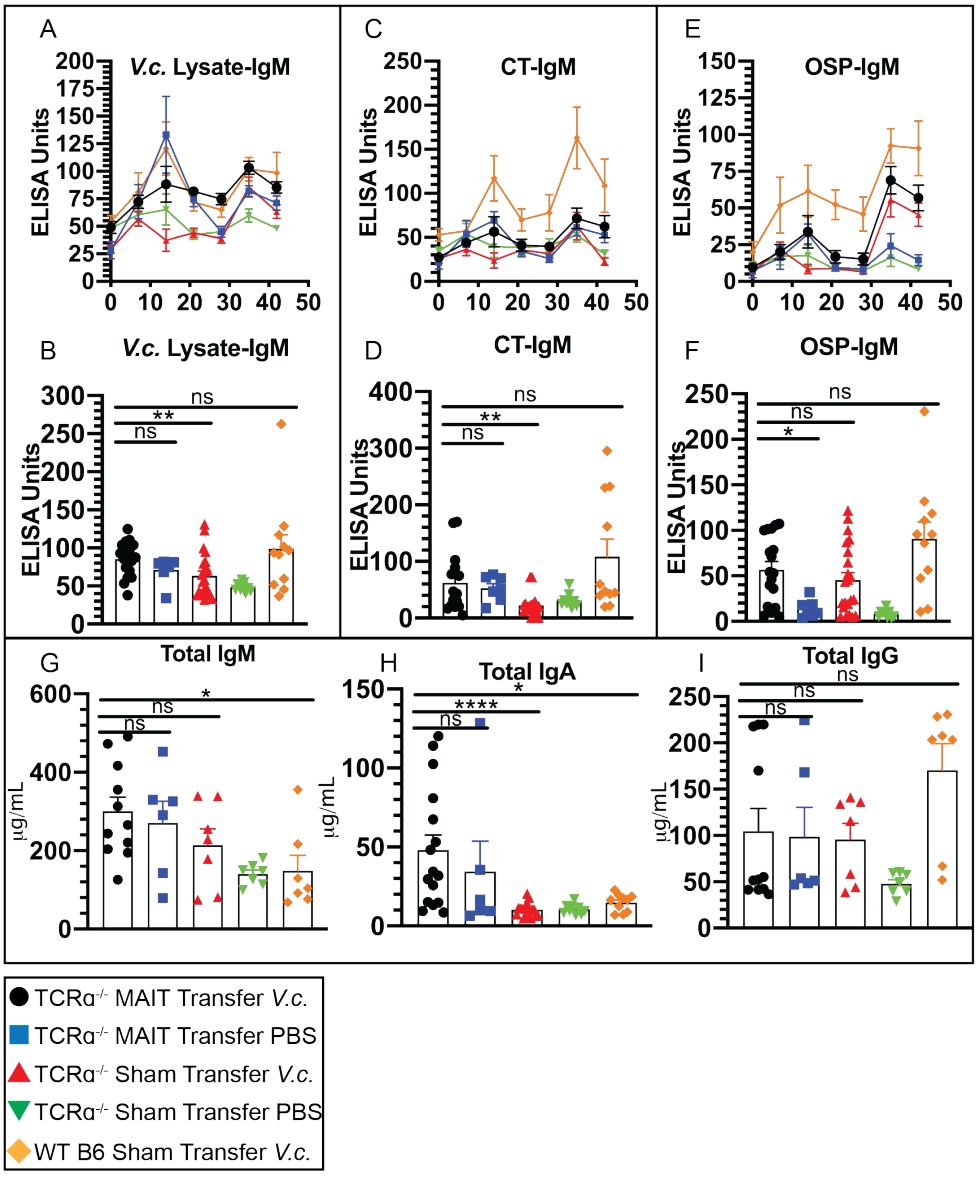

Supplementary Fig. 5. Serum IgM and total IgM, IgG and IgA ELISAs. (**A**-**F**) Serum *V. cholerae* lysate, OSP, and CT IgM ELISAs representing weekly antibody kinetics (**A, C** & **E**) and Day 42 endpoint responses (**B**, **D** & **F**). Data are represented as ELISA units normalized to a pooled serum positive control from WT B6 mice challenged with *V. cholerae*. Total IgM (**G**), IgA (**H**) and IgG (**I**) ELISAs from Day 42 endpoint serum. Total Ig was quantitated using a standard curve based on known Ig quantities. Data are represented as Mean with SEM from 5 independent experiments. n= 6-22 mice per group. $*p < 0.05$, $**p<0.01$, $***p<0.001$, $****p<0.0001$ by two-tailed Mann-Whitney *U* test. by two-tailed Mann-Whitney *U* test. Legend in black box denotes experimental groups.